

Role of Dynamin-2 in Muscle Development and Disease

by

Elizabeth M. Gibbs

A dissertation submitted in partial fulfillment
of the requirements for the degree of
Doctor of Philosophy
(Neuroscience)
in The University of Michigan
2012

Doctoral Committee:

Professor Eva L. Feldman, Chair
Professor John Y. Kuwada
Professor Henry L. Paulson
Professor Lois S. Weisman
Assistant Professor James Dowling

Muscles are in a most intimate and peculiar sense the organs of the will. They have built all the roads, cities and machines in the world, written all the books, spoken all the words, and, in fact done everything that man has accomplished with matter. Character might be a sense defined as a plexus of motor habits.

— G. Stanley Hall, 1907

© Elizabeth M. Gibbs

2012

Dedication

To my parents, for their unfailing enthusiasm and support

Acknowledgements

I owe a tremendous debt to the many people who have helped me along my graduate school path.

I have been extraordinarily lucky to have Dr. Eva Feldman as my mentor. She is an exceptional scientist and I have learned so much from her - both personally and professionally. Likewise, I am indebted to Dr. Jim Dowling, who has always been willing to share his expertise and enthusiasm. I am also grateful to Drs. Hank Paulson, Lois Weisman and John Kuwada for their encouragement and thoughtful criticism throughout my dissertation work.

It has been a privilege to work in both the Feldman and Dowling laboratories. It's hard to imagine a better training environment as graduate student, and I have been lucky to have to be surrounded by such a talented and diverse group of scientists. I am particularly grateful to Carey Backus and Arden Trickey-Glassman for their considerable moral support, in addition to expert technical assistance. I appreciate the guidance I have received through the Neuroscience Program, and I especially thank Valerie Smith for her help and friendship.

I have also been lucky to have an exceptional group of friends supporting me outside of the lab. Cindy Schoen and Adrienne Wang have helped make the past few years a joyful time, and I am grateful to have been able to share the ups and downs of graduate life with them. Likewise, I owe Natela Shanidze and Kevin Lim a great deal of thanks.

Much more than neighbors, they have become like family – a family with exceptional talent for copy-editing, home decorating and computer repair. Whatever the problem, I can always count on them for a sympathetic ear and sensible advice. I also thank Grace Lin for her constant encouragement, and Maia Krause for many years of friendship. I am grateful to Luvina, Brad and Wyatt Bowen for their love and support, and for continually reminding me of the most important things in life.

I owe Drs. Ginger Withers and Chris Wallace particular thanks for introducing me to neuroscience research, and for taking me under their wing as an undergraduate. Their continued friendship and encouragement during graduate school has meant a great deal to me. I am also very grateful to have been able to share my undergraduate and graduate years with Nancy Day, and I hope that our paths will continue to parallel over the decades to come.

Finally, I am truly grateful for the love and support of my family, especially my parents, John and Kate Gibbs. Their enthusiasm and encouragement has meant everything to me, and none this would have been possible without their support.

TABLE OF CONTENTS

Dedication.....	ii
Acknowledgements.....	iii
List of Figures.....	vii
Abstract.....	viii
Chapter 1: Introduction.....	1
1.1 DNM2 is a large GTPase with diverse roles in cellular function.....	2
1.2 Mutations in <i>DNM2</i> cause multiple forms of neuromuscular disease.....	4
1.3 Centronuclear myopathies are a clinically and genetically heterogeneous group of muscle disorders.....	8
1.4 Potential mechanisms of disease in DNM2-related centronuclear myopathy....	10
1.5 Murine models of DNM2-related centronuclear myopathy.....	17
1.6 Zebrafish as a model for neuromuscular disease.....	19
1.7 Summary of thesis.....	20
Chapter 2: Genomic organization and expression of two dynamin-2 genes in zebrafish.	23
2.1 Abstract.....	23
2.2 Introduction.....	23
2.3 Results.....	25

2.4	Discussion	33
2.5	Materials and Methods	35
Chapter 3: Neuromuscular junction abnormalities in DNM2-related CNM		38
3.1	Abstract	38
3.2	Introduction	39
3.3	Results	41
3.4	Discussion	50
3.5	Materials and Methods	53
Chapter 4: Alterations in excitation-contraction coupling in DNM2-related CNM		56
4.1	Abstract	56
4.2	Introduction	57
4.3	Results	59
4.4	Discussion	69
4.5	Materials and Methods	71
5	Conclusions and Future Directions.....	74
Bibliography		80

List of Figures

Figure 1-1: Mutations in DNM2 cause centronuclear myopathy.	8
Figure 1-2: Endocytic uptake is not altered in DNM2-S619L fibroblasts.....	12
Figure 1-3: Schematic of potential pathogenesis in DNM2-CNM	22
Figure 2-1: Phylogenetic and syntenic analysis of <i>dnm2</i> and <i>dnm2-like</i>	26
Figure 2-2: Molecular and protein structure of <i>dnm2</i> and <i>dnm2-like</i>	27
Figure 2-3: Spatial and temporal expression of <i>dnm2</i> and <i>dnm2-like</i>	28
Figure 2-4: Morpholino-mediated knockdown of <i>dnm2</i> and <i>dnm2-like</i>	29
Figure 2-5: Knockdown of <i>dnm2</i> and <i>dnm2-like</i> results in morphological changes.....	31
Figure 2-6: Human DNM2 RNA rescues <i>dnm2</i> and <i>dnm2-like</i> morphant phenotypes ...	32
Figure 3-1: Overexpression of DNM2-S619L causes a muscle-specific phenotype.....	42
Figure 3-2: DNM2-S619L larvae exhibit impaired motor function	44
Figure 3-3: Acetylcholine receptor distribution is disrupted in DNM2-S619L larvae....	46
Figure 3-4: AChEI treatment improves motor behavior in DNM2-S619L larvae.....	48
Figure 4-1: Motor deficits and muscle disorganization in <i>dnm2</i> knockdown fish.	60
Figure 4-2: <i>dnm2</i> knockdown disrupts membrane structure in muscle fibers.	62
Figure 4-3: Effects of DNM2 knockdown on DHPR localization.....	63
Figure 4-4: DNM2-S619L expression alters <i>ex vivo</i> tubulation in COS cells.....	65
Figure 4-5: T-tubule and SR abnormalities in DNM2-S619L larval muscle.....	66
Figure 4-6: Calcium activity in DNM2-S619L larvae muscle.....	68

Abstract

Centronuclear myopathies (CNMs) are a group of inherited muscle disorders characterized by muscle weakness and centralized nuclei on biopsy. Autosomal dominant centronuclear myopathy is caused by mutations in the gene encoding dynamin 2 (*DNM2*), a protein involved in endocytosis and membrane trafficking pathways. There is little known about the muscle dysfunction underlying this disorder, and there are currently no treatments.

The goal of this work is to gain greater insight into the role of DNM2 in normal muscle function and disease-related pathology. Since zebrafish muscle shares many features with higher vertebrates, we utilize zebrafish as a model system to characterize DNM2 function in muscle. We identify two zebrafish orthologs to human DNM2, and show that they are required for normal development. We further demonstrate that the knockdown of zebrafish *dnm2* results in a severe motor phenotype and that organization of t-tubules and sarcoplasmic reticulum (SR) is disrupted in these animals. To determine if these changes are relevant in the pathogenesis of DNM2-CNM, we establish a novel zebrafish model of DNM2-CNM by transiently overexpressing a mutant version of DNM2 (DNM2-S619L) during development. We show that overexpression of DNM2-S619L leads to histopathologic changes in muscle and a severe motor phenotype. We further demonstrate that the muscle weakness seen in these animals can be significantly alleviated by treatment with an acetylcholinesterase inhibitor, suggesting that abnormal neuromuscular transmission is involved in the pathology of DNM2-CNM. This finding

is supported by case histories of two patients with mutations in DNM2. In the muscle of DNM2-S619L fish, we also find substantial disorganization of the t-tubule and SR on muscle ultrastructure. DNM2-S619L overexpression in an *ex vivo* model of t-tubule formation provides additional evidence that CNM-associated mutations in DNM2 can disrupt t-tubule structure.

Together, our results suggest that deficits at the both the neuromuscular junction and sarcotubular network may play an important role in the pathogenesis of DNM2-CNM and that treatments targeting this dysfunction may provide disease-modifying therapies for patients with this disorder.

Chapter 1: Introduction

Intracellular membrane trafficking is essential in all cell types, but nerve and muscle cells present special demands on membrane trafficking pathways. This is reflected in the fact that mutations in many trafficking-associated genes cause a variety of neuromuscular disorders. Both neurons and myofibers are post-mitotic cells with highly specialized membrane structures, and mutations that disrupt membrane repair, recycling or turnover can lead to profound defects in nerve or muscle while leaving other tissue types unaffected.

One such gene is dynamin-2 (*DNM2*), which encodes a ubiquitously-expressed protein with critical functions in several membrane trafficking pathways. Mutations in *DNM2* cause two different neuromuscular disorders: Charcot-Marie-Tooth disease, a peripheral neuropathy, and centronuclear myopathy, a muscle disorder. While *DNM2* has a well-characterized role in endocytosis and related membrane trafficking pathways, the pathomechanisms underlying *DNM2*-related disease are largely unknown. Additionally, there is little known about the specific function of *DNM2* in nerve or muscle.

The work in this dissertation addresses the specialized role of *DNM2* in muscle and characterizes specific membrane abnormalities in a zebrafish model of severe *DNM2*-related centronuclear myopathy (*DNM2*-CNM). In this introduction, I outline the known

cellular functions of DNM and the pathology of DNM2-CNM. I also discuss the current understanding of disease mechanisms in centronuclear myopathies as a group, and describe some of the important animal models. Finally, I summarize the specific aims and findings of this dissertation.

1.1 DNM2 is a large GTPase with diverse roles in cellular function

Members of the dynamin superfamily are large GTPases with a wide range of cellular roles. The dynamin superfamily consists of classical dynamins and dynamin-like proteins [1]. Most of these proteins are involved in the fission or fusion of vesicles and organelles. Classical dynamins have a well-characterized role in the scission of budding vesicles during clathrin-mediated endocytosis, but they are also key players in a variety of other pathways. Classical dynamins participate in budding from the trans-Golgi network, phagocytosis, micropinocytosis, cytokinesis and centrosome cohesion [2-6]. They have also been shown to interact with many components of actin and microtubule networks, and may be involved in establishing cytoskeletal structures such as lamellipodia and focal adhesions [7-11].

In mammals, there are three classical dynamins: dynamin-1, dynamin-2 and dynamin-3. Dynamin-2 (DNM2) is expressed ubiquitously, while other genetic isoforms have restricted tissue expression [12, 13]. Dynamin-1 (DNM1) is expressed in the central nervous system [14]. The expression pattern of dynamin-3 (DNM3) has not been fully established, but it has been shown to be expressed in brain, testis, and lung [14, 15]. Although differentially expressed, these three classical dynamins are highly conserved, and they are believed to share the same basic function.

Dynamins were initially identified as microtubule-binding proteins [16]. It was later observed that dynamins oligomerize in helical formations around the necks of budding vesicles [17, 18]. Based on this finding, it has long been hypothesized that these dynamin assemblies serve to ‘pinch’ off budding vesicles in a GTP-dependent manner [19, 20]. The crystal structure of dynamin was recently solved [21, 22], providing a more precise understanding of how dynamin coordinates vesicle scission. These data support a model in which intermolecular interactions between dynamin domains facilitate a twisting motion of the dynamin assembly. This activity constricts and breaks the membrane, releasing the nascent vesicle.

The classical dynamins share five common domains: GTPase, pleckstrin homology (PH), middle, GTPase effector (GED) and proline rich (PRD) domains (Figure 1-1, A). Each of these regions has been shown to contribute to the endocytic function of dynamin. The GTPase domain serves to bind and hydrolyze GTP. The GED domain helps regulate this activity, and is also believed to coordinate dynamin self-assembly with the middle domain [23-25]. The PRD domain interacts with protein binding partners and assists in localizing dynamin to budding vesicles [26, 27].

The function of the dynamin PH domain is of particular interest, since many disease-associated mutations are located in this region. PH domains are typically characterized as phosphoinositide binding domains. The dynamin PH domain binds with high affinity to phosphatidylinositol-(4,5)-bisphosphate, an interaction which is believed to target dynamin to the plasma membrane [28-31]. However, recent evidence suggests that the dynamin PH domain does not simply act to localize dynamin molecules. Instead,

the PH domain may play a key role in facilitating GTPase activity, and its interaction with phosphoinositides could serve to regulate this function [32, 33].

1.2 Mutations in *DNM2* cause multiple forms of neuromuscular disease

Mutations in *DNM2* cause autosomal dominant centronuclear myopathy (DNM2-CNM) and Charcot-Marie-Tooth disease (DNM2-CMT). To date, 20 disease-causing mutations have been identified (Figure 1-1, A). The genotype-phenotype correlation between these mutations and disease remains unclear, although there are several residues that appear to be mutational hot spots. In 2005, the first mutations identified in DNM2-CMT and DNM2-CNM patients were restricted to the PH and middle domains, respectively [34, 35]. Since then, mutations causing both disorders have been found throughout the PH, middle and GED domains. Interestingly, there are several locations where a CMT-causing mutation is found within a few residues of a CNM-causing mutation.

1.2.1 DNM2-related centronuclear myopathy

Centronuclear myopathy is named for the characteristic biopsy finding in the disorder, a large numbers of muscle fibers with centralized nuclei (Figure 1-1, B and C). DNM2-CNM is usually characterized by a triad of histopathological findings: 1) a high percentage of muscle fibers with central nuclei, 2) type I fiber predominance, and 3) a radial organization of sarcoplasmic strands on oxidative staining.

Patients with DNM2-CNM typically present with either a severe or moderate disease course. In the moderate form, patients develop slow progressive symptoms and may not be diagnosed until adulthood. If symptoms are present in childhood, they may

include exercise-induced myalgia, difficulties running or walking, and frequent ankle sprains. Weakness most often presents in the distal muscles, although proximal muscles may also be affected. Patients usually have facial and extraocular weakness, and ptosis is frequently present. Patients may develop contractures and scoliosis. Of particular clinical importance, a number of patients with respiratory involvement have been reported [36-39]. Reports that even mildly-affected patients may develop restrictive respiratory syndrome suggest that this is a significant feature of the disease.

In the severe form of CNM, patients exhibit significant weakness at birth. Infants with severe DNM2-CNM frequently require nasogastric feeding and respiratory support. Motor milestones may be substantially delayed, such as head control, sitting unsupported and walking. Joint contractures are present in the majority of reported patients. Interestingly, patients with severe DNM2-CNM are often reported to improve substantially in the first few years of life, and patients with genetically-confirmed DNM2-CNM are usually able to walk by early childhood. For some patients, this improvement seems to decline in late childhood and early adolescence, when patients may lose ambulation and develop more severe respiratory problems. The long-term prognosis for patients with severe DNM2-CNM is currently unknown. As more patients with DNM2 mutations are identified, it will be important to carefully examine the disease course associated with both moderate and severe DNM2-CNM.

Several non-muscle features have been reported in patients with DNM2-CNM. A few patient cohorts present with congenital neutropenia, a condition that is also seen in some patients with DNM2-CMT [34, 40, 41]. It has also been suggested that DNM2-CNM can have central or peripheral nervous system involvement, although this remains

controversial. While most patients are intellectually normal, some patients exhibit mild cognitive impairment [39, 42, 43]. In term of peripheral involvement, it has been reported that some patients exhibit EMG patterns that suggest nerve involvement [42, 43]. Ultrastructural data from one patient also showed thinning of the myelin in peripheral nerve [44]. In view of the proximity of CNM- and CNM- causing mutations in *DNM2*, it will be important for future studies to establish overlap between these two disorders.

1.2.2 *DNM2*-related Charcot-Marie-Tooth disease

While the research in this dissertation is focused on understanding *DNM2*-CNM, it is worthwhile to discuss some features of the peripheral neuropathy associated with *DNM2* mutations. *DNM2*-CMT is characterized by slow progressive muscle weakness and atrophy, as well as varying degrees of sensory loss. Disease progression is usually relatively mild, and most patients retain ambulation [45].

Mutations in dozens of genes can cause different subtypes of Charcot-Marie-Tooth disease. Based on electrophysiological examination, CMTs can be categorized as axonal or demyelinating. To date, patients with *DNM2*-CMT have been reported to have two different forms of CMT: axonal and dominant intermediate, a rare form of CMT with features of both axonal and demyelinating neuropathy. Patients with *DNM2*-CMT have not been reported to exhibit myopathic features.

As with *DNM2*-CNM, some patients with *DNM*-CMT exhibit a few non-neurologic features. A mild congenital neutropenia co-segregates with CMT in several families [34, 41]. Interestingly, cataracts have also been reported in several patients with

DNM2-CMT or DNM2-CNM [41, 46], suggesting that DNM2 might have a role in maintaining lens transparency. It is unclear if these non-muscle pathologies are linked to specific DNM2 mutations, and further study is needed to determine their prevalence.

1.2.3 Expanded spectrum of DNM2-related diseases

In light of DNM2's importance in several critical aspects of cellular function, it is surprising that mutations in DNM2 cause disorders that only affect one cell type. In the past 5 years, however, it has become clear that DNM2 mutations can cause a wide spectrum of neuromuscular phenotypes that largely spare other tissues and organs. Myopathy patients with centralized nuclei on muscle biopsy and possible autosomal dominant inheritance should be considered for DNM2 screening regardless of disease severity. Likewise, CMT patients with dominant intermediate features on nerve conduction studies should be screened for possible DNM2 mutations, particularly if neutropenia is also present.

In addition to neuromuscular disorders, it is worth considering DNM2 as a causative gene for congenital neutropenias and early-onset cataracts in the absence of apparent myopathic or neuropathic features. Several patients with DNM2-CMT were reported to have low neutrophil counts prior to complaints of muscle weakness [34]. One neutropenic patient with DNM2-CNM presented with no muscle weakness, despite prominent centralized nuclei on biopsy [40]. In view of the highly variable neurologic phenotypes seen in patients with DNM2-CNM and DNM2-CMT, it may be informative to screen for DNM2 mutations in patients with congenital neutropenia without overt muscle symptoms. It is possible that DNM2 will be identified as a causative gene for

additional non-neuromuscular disorders, expanding the spectrum of DNM2-related diseases.

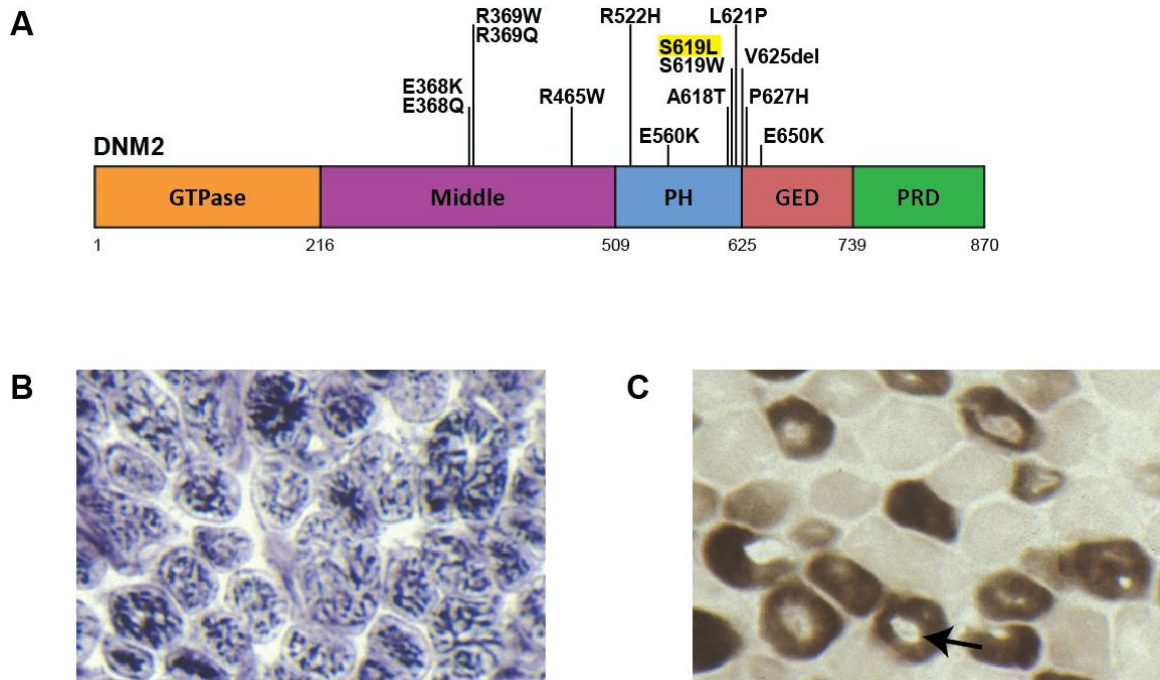


Figure 1-1: Mutations in DNM2 cause centronuclear myopathy.

(A) Protein structure of DNM2, with the location of CNM-associated mutations marked. The mutation studied in this dissertation, DNM2-S619L, is highlighted. (B) Muscle biopsy from a patient with a DNM2-S619L mutation, displaying irregular NADH-TR staining. (C) Muscle biopsy stained for ATPase (pH 4.2), highlighting type I fibers. Arrow points to centralized nucleus.

1.3 Centronuclear myopathies are a clinically and genetically heterogeneous group of muscle disorders

In addition to DNM2, mutations in three other genes been shown to cause centronuclear myopathy: *BINI*, *MTM1*, and *RYR1*. The purpose of this section is to give a brief introduction to these disorders, and to describe the associated genes.

1.3.1 Myotubular myopathy

Myotubular myopathy is an X-linked form of centronuclear myopathy caused by mutations in the myotubularin gene (*MTMI*) [47]. Myotubularin is a phosphoinositide phosphatase implicated in endosome sorting and maturation [48, 49]. Myotubular myopathy is the most common and most severe subtype of centronuclear myopathy. Infants typically present with severe muscle weakness and hypotonia at birth, and death in the first year of life is not uncommon [50]. Patients with the disorder frequently require respiratory support and most will never achieve independent ambulation [50-52].

1.3.2 BIN1-related centronuclear myopathy

Mutations in *BINI* cause a rare form of recessive centronuclear myopathy, which has so far been identified in only a few patients [53-56]. The clinical course of this disease is not well-characterized, but patients described in the literature all displayed moderate and progressive muscle weakness starting in infancy or childhood [36]. Muscle biopsies from patients with *BINI* mutations have similar histopathologic changes to DNM2-CNM muscle, and some fibers show the same distinctive radial sarcoplasmic strands on oxidative staining [57]. *BINI* encodes the protein amphiphysin 2, which plays an important role in sensing and shaping membrane curvature during endocytosis and other trafficking pathways. Of note, amphiphysin-2 binds to DNM2 during clathrin-mediated endocytosis [58], and several CNM-causing mutations in *BINI* have been shown to disrupt this interaction [53].

1.3.3 Ryanodine receptor-related centronuclear myopathy

Mutations in the ryanodine receptor (*RYR1*) have recently been identified in sporadic cases of centronuclear myopathy [59, 60]. The ryanodine receptor is a 560 kDa

calcium channel with a critical role in muscle contraction. Intriguingly, mutations in *RYR1* cause several other disorders, including malignant hypothermia susceptibility (MHS), central core disease, multi-minicore disease and King-Denborough syndrome. Mutations in *RYR1* have also been identified in a cohort of seven patients with an unnamed congenital myopathy characterized by muscle weakness and internalized nuclei on biopsy [61].

1.3.4 Uncharacterized centronuclear myopathies

There are still many patients with genetically uncharacterized centronuclear myopathies. The identification of additional genes will provide important insight into the cellular pathways involved in these disorders. It also remains to be seen what factors influence disease severity. There is evidence that polymorphisms in *MTMR14*, a member of the myotubularin family, may play a role in modulating the severity of disorder in some patients [62]. In a zebrafish model of myotubular myopathy, concurrent knockdown of zebrafish *mtm14* significantly exacerbates muscle phenotype [63, 64]. The extent of the role of *MTMR14* in centronuclear myopathy pathology is unknown; however, these findings suggest that additional genes may influence disease progression in some patients.

1.4 Potential mechanisms of disease in DNM2-related centronuclear myopathy

There is currently little known about the specific cellular dysfunction that leads to muscle weakness in DNM2-CNM. However, there have been important advances in the genetic understanding of other centronuclear myopathy subtypes in the past few years, and several animal models have been established for these disorders. These advances have provided important insights into the pathomechanisms that might underlie DNM2-

CNM. In this section, I will describe the results of cellular and *in vitro* studies of CNM-associated mutations in DNM2. I will also discuss evidence for membrane defects at two key regions of the myofiber: the neuromuscular junction (NMJ) and the t-tubule/sarcoplasmic (sarcotubular) region. These findings have been primarily drawn from studies of myotubular myopathy animal models and patients with non-DNM2-linked centronuclear myopathy.

1.4.1 Clathrin-mediated endocytosis and DNM2-related centronuclear myopathy

Given the central role of DNM2 in clathrin mediated endocytosis – and the fact that the gene product of *BIN1* is also involved in this pathway - a number of groups have considered the possibility that disease-associated mutations in DNM2 could interfere with cellular uptake. To date, studies examining the effect of these mutations on clathrin-mediated endocytosis have given conflicting results. Endocytic defects have been reported in several DNM2 mutations associated with CMT [34, 65]. Bitoun et al. showed that uptake of two endocytic markers was inhibited in cells overexpressing mutant dynamin constructs (R465W, K562E, V225del and E650K mutations) [66]. Likewise, Koutsopoulos et al. reported a decrease in endocytic uptake when they examined cells overexpressing additional CNM- and CMT- associated mutations (G358R, R465W, R522H, K562E, S619L and P627H mutations) [67].

By contrast, Lui et al. did not find alterations in clathrin-mediated endocytosis when they looked at mutant DNM2 constructs expressed in fibroblasts from *Dnm2* knockout mice (E368K, R465W, L570H and D555-E557del mutations) [68]. They did note impairment in other clathrin-independent pathways. This raises the possibility that the previously observed defects may depend on overexpressing mutant DNM2 in cells

with normal levels of endogenous DNMT2.; there is evidence that overexpression of even wild-type DNMT2 can result in aberrant cellular activity [69]. In support of these findings, Koutsopoulos et al. did not find a decrease in endocytic uptake in fibroblasts from two patients with R465W or S619L mutations [67]. This is consistent with unpublished data from our lab. We examined transferrin uptake in fibroblasts from a patient with an S619L mutation, and we found no difference in transferrin uptake between control human fibroblasts and fibroblasts from the patient (Figure 1-2, A and B).

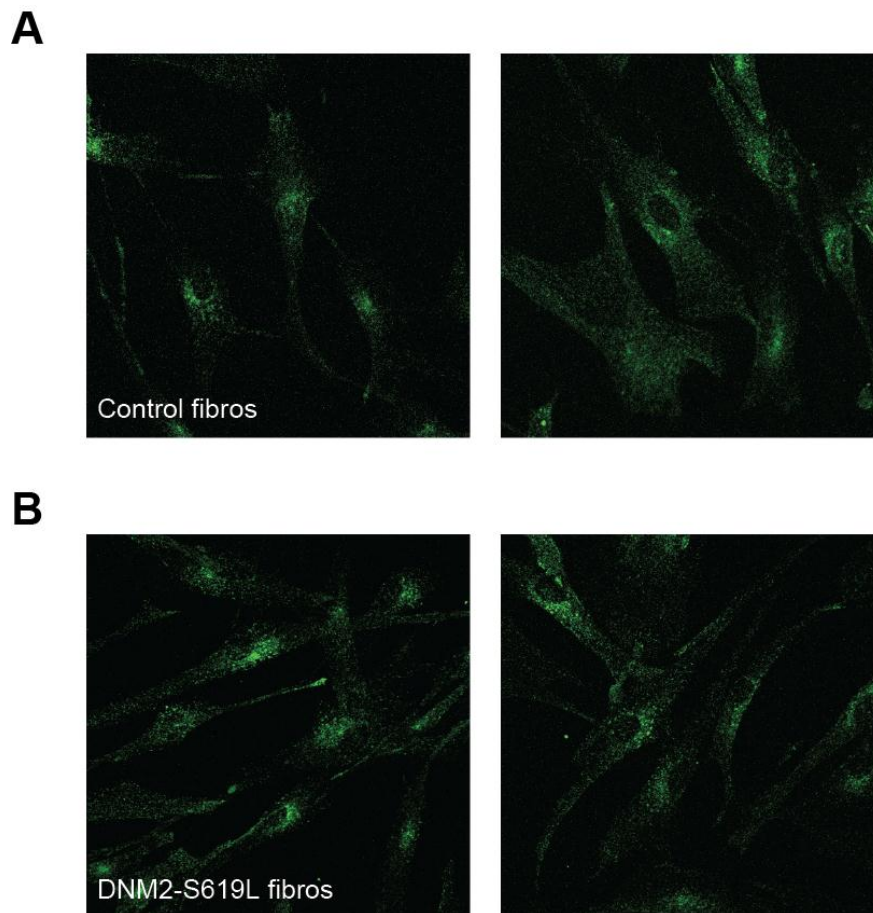


Figure 1-2: Endocytic uptake is not altered in DNMT2-S619L fibroblasts

Control and patient fibroblasts were serum-starved and treated with fluorescently labeled transferrin for 15 min at 37°C. We saw no difference in transferrin uptake between control and patient fibroblasts.

Some of these discrepancies may be due to the different methodologies and cell types used across these studies. It is also possible that there is a functional difference between certain CNM-associated mutations, and that some of the inconsistencies in these studies reflect fundamental differences in mutant activity. Given that known mutations in *DNM2* cause a phenotype specific to muscle and nerve, it seems reasonable to assume that the effect of these mutations will be subtle and may not significantly disrupt basal pathways in non-muscle cells. In order to better understand *DNM2* mutations in a disease context, it will be important for future studies to examine any putative trafficking defects in myofibers.

1.4.2 In vitro studies of DNM2-CNM mutations

Although most studies of *DNM2*-CNM have focused on alterations in cellular pathways, two recent *in vitro* studies examined the biochemical properties of mutant *DNM2* protein. These papers provide the first direct evidence for disease-associated changes in the physical activity of dynamin molecules, and they provide important insight into the molecular basis of the disease. Wang et al. examined 4 mutations associated with *DNM2*-CNM or *DNM2*-CMT (E68K, R369W, R465W and A618T mutations) [70]. They found that these mutant proteins increased GTPase activity relative to wild type *DNM2*, and that mutant dynamin oligomers are less prone to disassembly. Similarly, Kenniston et al. found that several PH domain mutations also increase GTPase activity [71]. Importantly, they also show that these mutations do not alter phosphoinositide binding, which has been widely suggested to be a molecular mechanism of disease in *DNM2*-CNM. Instead, these data imply that PH domain mutations can alter dynamin's response to phosphoinositide stimulation.

Taken together, these findings provide important new insights into the nature of CNM-causing mutations in DNM2. Much discussion of DNM2-related disease has rested on the assumption that these mutations inhibit clathrin-mediated endocytosis or another dynamin-related pathway. These two papers provide the first evidence that disease-associated mutations can instead increase DNM2 activity. They also suggest that these mutations might disrupt the interplay between the lipid membrane and dynamin molecules, causing dysregulation of GTPase activity and oligomerization. Rather than altering binding affinity, CNM-associated mutations in the PH domains may alter activity through the decoupling of complex regulatory mechanisms that govern DNM2 activity.

1.4.3 T-tubule structure and centronuclear myopathy

Recent evidence suggests that abnormalities in t-tubule structure are shared in several genetic subtypes of centronuclear myopathy. T-tubules are deep invaginations of the plasma membrane, which conduct electrical excitation into the interior of the cell. These membrane structures are closely aligned with the sarcoplasmic reticulum (SR), a network of specialized endoplasmic reticulum which releases calcium. The interaction between t-tubules and SR is responsible for excitation-contraction (EC) coupling – the translation of an electrical stimulus into a muscle contraction. When an action potential is propagated across the myofiber, voltage-sensitive proteins in the t-tubule trigger the release of calcium from the SR. Together, these two membrane structures mediate downstream muscle contraction and relaxation through the rapid release and uptake of calcium.

The identification of CNM-causing mutations in *BINI* provided the first significant evidence that disruption in t-tubules might be a component of pathology in

centronuclear myopathy. The gene product of *BINI* had previously been shown to be critical for the biogenesis of t-tubules [72, 73]. In the initial characterization *BINI*-associated centronuclear myopathy, Nicot et al. showed that expression of mutant protein disrupted tubulation in an *ex vivo* model of t-tubule formation [53]. More recently, studies have shown abnormal organization of t-tubule and defects in EC coupling in three different animal models of MTM1-CNM [74-76]. Dowling et al. 2009 showed ultrastructural abnormalities in three patients with myotubular myopathy [74], and a number of studies have shown mislocalization of triad markers on biopsies from patients with MTM1-CNM, DNM2-CNM or BIN1-CNM [53, 57, 74]. Further study is needed to establish the prevalence and pathological significance of these findings, but current evidence suggests that sarcotubular defects may be a common defect among genetically distinct forms of centronuclear myopathy.

1.4.4 Evidence for a defect at the neuromuscular junction

In addition to the emerging evidence for t-tubule disruption in centronuclear myopathies, there is evidence in the literature that some patients with centronuclear myopathy may also have defects at the neuromuscular junction (NMJ). An early report of centronuclear myopathy in two adolescent siblings noted elongation of endplates on muscle biopsy [77]. Similar endplate abnormalities have been described in at least two other case reports: endplate elongation on teased muscle fibers from a 67 year old woman with late onset centronuclear myopathy [78] and irregular extended acetylcholinesterase staining on muscle fibers from an infant with severe centronuclear myopathy [79]. An ultrastructural study of muscle from another severely affected infant found that post-

synaptic junctional folds were irregular and unelaborated [80], consistent with findings in some congenital myasthenias [81].

Two recent studies provide further support for NMJ involvement in some patients with centronuclear myopathy. Liewluck et al. described a patient with genetically uncharacterized centronuclear myopathy combined with clinical and electrophysiological features of myasthenia [82]. They found histological abnormalities at the post-synaptic membrane consistent with previous reports, including irregular acetylcholinesterase staining, reduced acetylcholine receptor staining and, at the ultrastructural level, underdeveloped junctional folds. *In vitro* electrophysiology on isolated muscle suggested both a pre- and post-synaptic deficiency in affected NMJs. Similarly, Robb et al. reported three patients with genetically uncharacterized centronuclear myopathy and one patient with myotubular myopathy [83]. These patients exhibited fatigability and abnormal jitter on EMG. All four patients responded favorably to acetylcholinesterase inhibitor treatment, and two patients showed substantial improvement with sustained therapy. In this same report, a zebrafish model of myotubular myopathy was shown to have acetylcholine receptor patterning. Motor weakness in these animals was also partially alleviated by acetylcholinesterase inhibitor treatment.

Taken together, these case reports provide intriguing evidence that NMJ defects might play a role in the pathogenesis of centronuclear myopathies. However, this aspect of disease has been examined in very few patients with a genetically defined disorder. Further study is needed to establish the prevalence of NMJ abnormalities in genetically distinct forms of centronuclear myopathy.

1.5 Murine models of DNM2-related centronuclear myopathy

As described above, most investigations of DNM2-CNM have examined mutant DNM2 function in non-muscle cell culture or biochemical assays. Until recently, studies in muscle have been limited by a lack of animal models for DNM2-CNM. However, in the past year, descriptions of two murine models of DNM2-CNM have been published: a DNM2-R465W knock-in mouse and a model utilizing DNM2-R465W viral overexpression in mouse muscle [84, 85]. The characterization of both models has expanded the repertoire of tools to study centronuclear myopathies. However, both of these systems have some important limitations in their ability to model DNM2-CNM. In this section, I will address the strengths and weaknesses of both mouse models.

1.5.1 DNM2-CNM mouse knock-in model

The middle domain R465W mutation is associated with a moderately mild familial form of DNM2-CNM, and it is the most common DNM2 mutation currently described in the literature [35, 38, 44]. Durieux et al. introduced the R465W mutation into the endogenous mouse *Dnm2* [85]. Surprisingly, these heterozygous R465W knockin mice exhibit no motor phenotype or reduction in lifespan, although most homozygous mice die within 24 hours of birth. Maximal force measurements of heterozygous muscle revealed a reduction in force generation by three weeks of age. There is mild atrophy of the tibialis anterior at 2 months, and the size of two other muscle groups is modestly decreased by 8 months.

Of note, heterozygous DNM2-R465W mice do not share any of the major histopathological findings in DNM2-CNM patient muscle. There is no alteration in nuclei position and there are no ultrastructural abnormalities. Interestingly, an abnormal

clustering of dysferlin and DNM2 is seen in some muscle fibers, and the authors demonstrate similar dysferlin distribution on muscle biopsies from four patients with DNM2-CNM. This novel finding suggests that muscle fibers from R465W mice may share subtle pathologic changes with DNM2-CNM, despite an overall lack of disease phenotype.

1.5.2 Viral overexpression in mouse muscle

In a non-genetic mouse model of DNM2-CNM, Laporte et al. overexpressed DNM2-R465W in adult tibialis anterior muscle using adeno-associated virus injection [84]. After 2 weeks, injected muscle shows histopathological features similar to those of DNM2-CNM: centralized nuclei, fiber atrophy and abnormal oxidative staining. They also note strikingly misoriented t-tubules, as well as mild irregularities in t-tubule shape and swollen sarcoplasmic reticulum.

The overexpression strategy used to generate DNM2-R465W muscle in this study has several inherent limitations. First, expression of the mutant construct is restricted to only one muscle. This precludes the characterization of some phenotypic changes that would be evident in a whole-animal model, such as survival and motor behavior. Second, DNM2-R465W expression is induced in adult muscle, which would not reveal any effect that the mutant protein has on muscle development. However, the fact that these mice develop a robust CNM-like phenotype demonstrates an important fact that would not be evident in a transgenic or knockin model: DNM2-R465W can cause substantial defects in muscle after myogenesis has been fully completed. This model has provided important insight into the pathogenesis of DNM2-CNM and it promises to be extremely useful for future studies.

1.6 Zebrafish as a model for neuromuscular disease

In recent years, zebrafish have emerged as a useful developmental and genetic model. Several factors make zebrafish particularly appealing. Zebrafish have a short reproductive cycle and a single breeding pair can lay hundreds of eggs in one day. Zebrafish embryos develop quickly and can be genetically or pharmacologically manipulated with relative ease. In combination with large clutch size, the rapid development of zebrafish embryos makes them an excellent system for high-throughput drug or mutational screens. Embryos are also transparent, which allows many cellular and developmental events to be observed *in vivo*.

1.6.1 Zebrafish models of human muscle disease

Zebrafish offer several specific advantages as a model for human muscle disorders. The zebrafish neuromuscular system has been extensively studied, and early locomotor behavior has been well characterized. Skeletal muscle develops quickly in the zebrafish - by 24 hours of development, embryos already have developing muscle fibers. Skeletal muscle is very prominent in embryos and larvae, and due to the transparency of the developing fish, individual myofibers can be easily observed. Additionally, zebrafish muscle shares many molecular and histological features with mammalian muscle.

Zebrafish have been successfully used to model several human muscle disorders. A zebrafish model of myotubular myopathy is particularly relevant to the work described in this dissertation. Dowling et al. demonstrated that knockdown of zebrafish myotubularin results in a phenotype that shares many key features of human myotubular myopathy: motor defects, abnormalities in muscle nuclei positioning, hypotrophic myofibers and EC coupling defects [63, 74]. This model provided the first evidence that

EC coupling defects are a significant feature of myotubular myopathy, which has since been demonstrated in murine and canine models [75, 76]. As previously discussed, T-tubule abnormalities have also been identified in patients with myotubular myopathy [57, 74]. The translation of these findings from fish to human demonstrate that zebrafish can provide a powerful system for examining muscle dysfunction in centronuclear myopathies.

1.7 Summary of thesis

Mutations in *DNM2* cause an autosomal dominant centronuclear myopathy characterized by moderate to severe muscle weakness. There is little known about the specific mechanisms that lead to this muscle weakness and there are currently no disease-modifying therapies. **This dissertation will examine the hypothesis that CNM-linked mutations in *DNM2* disrupt the organization of key membrane components associated with neuromuscular transmission and EC coupling.**

Specific Aim 1: Identify and characterize zebrafish orthologs to human *DNM2*. There are no published studies characterizing classical dynamins in the zebrafish genome. In light of the key role dynamin-2 plays in mammalian cell function and human disease, understanding the zebrafish dynamin-2 homolog is important. In Chapter 2, I present work identifying two highly conserved zebrafish orthologs to human *DNM2*, and I demonstrate that knockdown of either ortholog perturbs normal development.

Specific Aim 2: Characterize neuromuscular junction changes in a zebrafish model of *DNM2*-CNM. As described in Section 1.5, current mouse models for *DNM2*-CNM are unable to provide an organism-wide phenotype that recapitulates the human disorder. To

address this gap, I generated a transient zebrafish model overexpressing human DNM2-S629L. In Chapter 3, I show that these fish exhibit pronounced motor defects and abnormal clustering of neuromuscular junctions. I further demonstrate that these motor defects can be dramatically alleviated by treatment with acetylcholinesterase inhibitors. Together, these data suggest that defects in neuromuscular transmission contribute to muscle pathology in DNM2-CNM fish.

Specific Aim 3: Characterize EC-coupling machinery in a *dnm2*-deficient zebrafish and a zebrafish model of DNM2-CNM. There is growing evidence that EC coupling defects are a common feature of centronuclear myopathies; however, this has not been extensively examined in DNM2-CNM. To better understand the role of DNM2 in establishing and maintaining membrane structures associated with EC coupling, I examined ultrastructure and triad markers in two different zebrafish models: zebrafish with reduced *dnm2* expression and zebrafish overexpressing human DNM2-S619L. Although *dnm2* does not seem to be a requirement for primary t-tubule biogenesis, as has been previously suggested, *dnm2* deficiency causes substantial abnormalities in the general organization of the t-tubule and sarcoplasmic reticulum. Similarly, DNM2-S619L fish exhibit striking disorganization of these sarco-tubular membranes. Finally, I demonstrate that these fish have reduced spontaneous calcium transients, indicating a functional defect in EC coupling.

Taken together, these findings point to two potential pathogenic changes in DNM2-CNM. They also reveal a class of therapeutics, acetylcholinesterase inhibitors, that may benefit patients with this disorder. Collectively, these studies provide important

insight into the pathomechanisms underlying muscle weakness in DNM2-CNM and will contribute towards a deeper understanding of the centronuclear myopathies as a whole.

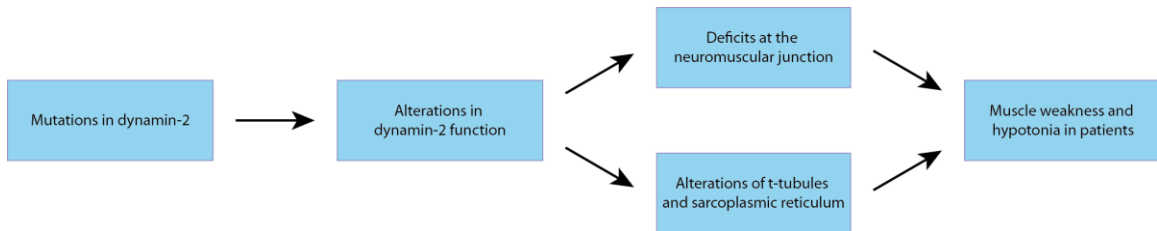


Figure 1-3: Schematic of potential pathogenesis in DNM2-CNM

Our results support a model of disease in which two fundamental changes contribute to muscle weakness: deficits in neuromuscular transmission and alterations of the sarcotubular network.

Chapter 2: Genomic organization and expression of two dynamin-2 genes in zebrafish

2.1 Abstract

Dynamin-2 (DNM2) is a large GTPase involved in clathrin-mediated endocytosis and related trafficking pathways. Mutations in *DNM2* cause two distinct neuromuscular disorders: centronuclear myopathy and Charcot-Marie-Tooth disease. Zebrafish have been shown to be an excellent animal model for many neurologic disorders, and this system has the potential to inform our understanding of DNM2-related disease.

Currently, little is known about the endogenous zebrafish orthologs to human *DNM2*. In this study, we characterize two zebrafish dynamin-2 genes, *dnm2* and *dnm2-like*. Both these orthologs are structurally similar to human DNM2 at both the gene and protein levels. They are expressed throughout early development, and we also detected expression in all adult tissues examined. Knockdown of *dnm2* and *dnm2-like* gene products resulted in extensive morphological abnormalities during development, and expression of human RNA rescued these phenotypes. Our findings suggest that *dnm2* and *dnm2-like* are true orthologs to human *DNM2*, and that they are required for normal zebrafish development.

2.2 Introduction

Dynamins are large GTPases involved in a wide range of cell and organelle fission events. The dynamin superfamily is made up of classical dynamins and dynamin-like

proteins. Classical dynamins are critical components of clathrin-mediated endocytosis, where they contribute to the release of newly formed endosomes [21, 22, 86]. In addition to this well-characterized role in endocytosis, classical dynamins participate in a variety of membrane trafficking functions including phagocytosis, caveolae internalization and trans-Golgi transport [2, 3, 87].

Currently, there is no published characterization of any classical dynamin in the zebrafish genome. In mammals, there are three classical dynamins: dynamin-1, dynamin-2, and dynamin-3. Of these three genetic isoforms, only dynamin-2 (DNM2) is ubiquitously expressed [12-14]. A requirement for DNM2 during development is evidenced by an embryonic lethal phenotype in DNM2 knockout mice [10]. Mutations in human *DNM2* also cause two different neuromuscular disorders, Charcot-Marie-Tooth disease and centronuclear myopathy [34, 35]. Given the prominent role of DNM2 in cellular function and human disease, characterizing the endogenous zebrafish dynamin-2 is an important task. Several studies of zebrafish endocytosis have utilized putative markers of dynamin-2; however, none of these reports examined the functional or structural similarity between human DNM2 and a zebrafish homolog [88-90]. Establishing this orthologous relationship will enable future studies of endocytosis and other dynamin-related pathways in the zebrafish.

In this chapter, we characterize two zebrafish dynamin-2 genes, *dnm2* and *dnm2-like*. We demonstrate that *dnm2* and *dnm2-like* are structurally similar to human DNM2 at both the gene and protein levels, and that, like mammalian dynamin-2 proteins, they are ubiquitously expressed. Using morpholino-mediated knockdown, we show that depletion of *dnm2* and *dnm2-like* gene products causes morphological abnormalities

during development. Taken together, this evidence suggests that *dnm2* and *dnm2-like* are both structural and functional orthologs to human *DNM2*, and that they are required for normal embryonic development in the zebrafish.

2.3 Results

2.3.1 Identification of two *dnm2* genes in zebrafish

Using public databases (NCBI, ENSEMBL, ZFIN) and RACE PCR, we identified two separate zebrafish genes highly related to human *DNM2* on chromosomes 3 and 1 (Figure 2-1, A; Genbank ID559334 and ID 406525; zfin zgc:114072 and zgc:77233). 3' RACE PCR on *dnm2* identified an additional 3 exons not included in any databases. These exons shared sequence homology with the 3 final exons in human *DNM2* and zebrafish *dnm2-like*.

Table 1: Comparison of zebrafish dynamin-2 genes with human classical dynamins

	<i>dnm1</i> (Dr)	<i>dnm2</i> (Dr)	<i>dnm3</i> (Dr)	<i>dnm2-like</i> (Dr)	<i>DNM1</i> (Hs)	<i>DNM2</i> (Hs)	<i>DNM3</i> (Hs)
<i>dnm1</i> (Dr)	100% (843)	81% (762)	72% (845)	77% (849)	88% (847)	67% (875)	78% (847)
<i>dnm2</i> (Dr)		100% (755)	79% (753)	89% (752)	83% (763)	88% (757)	83% (757)
<i>dnm3</i> (Dr)			100% (825)	73% (847)	73% (849)	74% (859)	77% (840)
<i>dnm2-like</i> (Dr)				100% (856)	78% (848)	81% (874)	78% (869)
<i>DNM1</i> (Hs)					100% (864)	79% (857)	80% (848)
<i>DNM2</i> (Hs)						100% (870)	80% (874)
<i>DNM3</i> (Hs)							100% (859)

Percent identity was determined by BLASTP. The length of homologous overlap is in parenthesis (number of amino acids).

We additionally screened these databases for zebrafish genes with high sequence homology to other human classical dynamins. Comparison of the two putative zebrafish dynamin-2 genes with human dynamins revealed that both zebrafish genes share highest sequence homology with human *DNM2* (Table 1). Phylogenetic analysis also grouped

both genes into the *DNM2* cluster (Figure 2-1, B). Analysis of genes surrounding the human *DNM2* revealed a conserved syntenic cluster including the *dnm2* gene on zebrafish chromosome 3 (Figure 2-1, C).

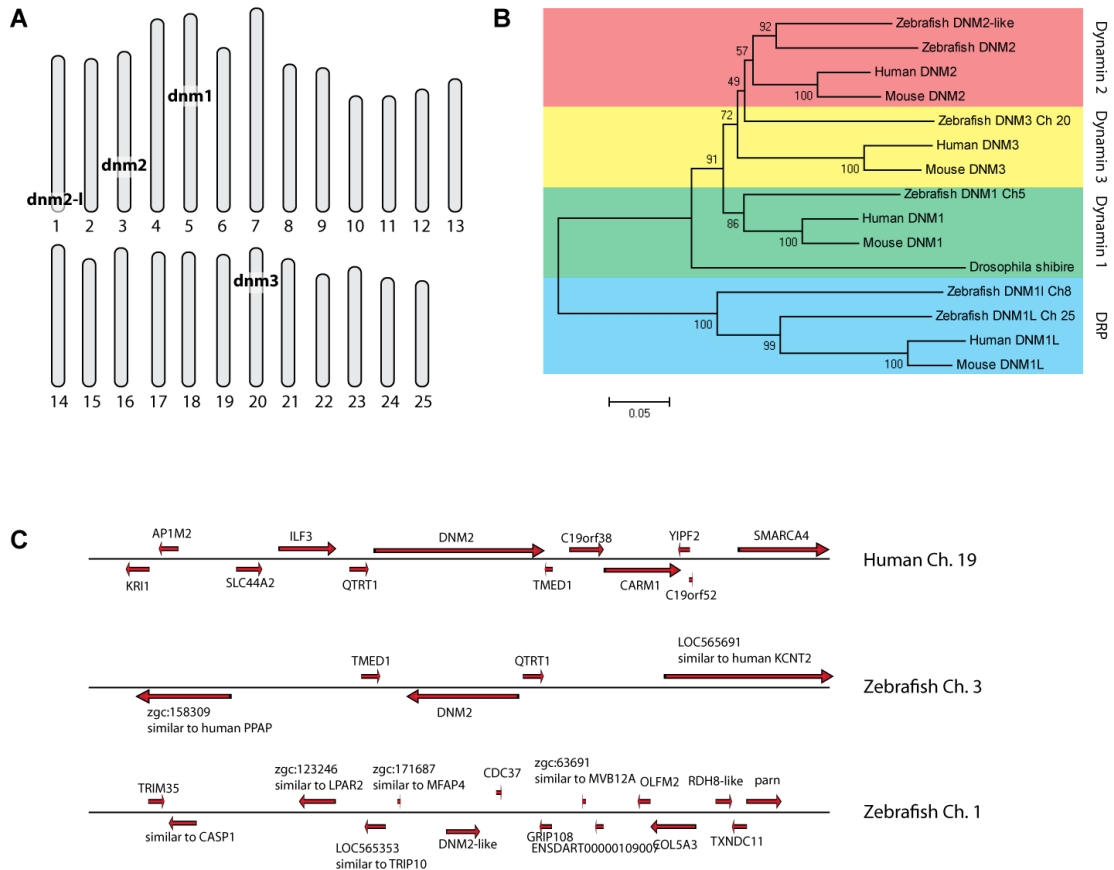


Figure 2-1: Phylogenetic and syntenic analysis of *dnm2* and *dnm2-like*

(A) Chromosomal locations of zebrafish homologues to human DNM1, DNM2 and DNM3. (B) Phylogenetic tree comparing dynamitin-2 genes in multiple species. (C) Syntenic organization of human DNM2 compared with zebrafish *dnm2* and *dnm2-like*.

Both zebrafish proteins share all five major domains of human DNM2, including a GTPase domain, a GTAase effector domain (GED), a dynamin-specific middle domain, a pleckstrin homology (PH) domain and a PRD domain. At the protein level, these domains all share close identity with the domains of human DNM2 (Figure 2-2, B). The two zebrafish *dnm2* genes also share similar intron-exon organization with human *DNM2*, although *dnm2-like* has substantially smaller introns than either other gene (Figure 2-2, A).

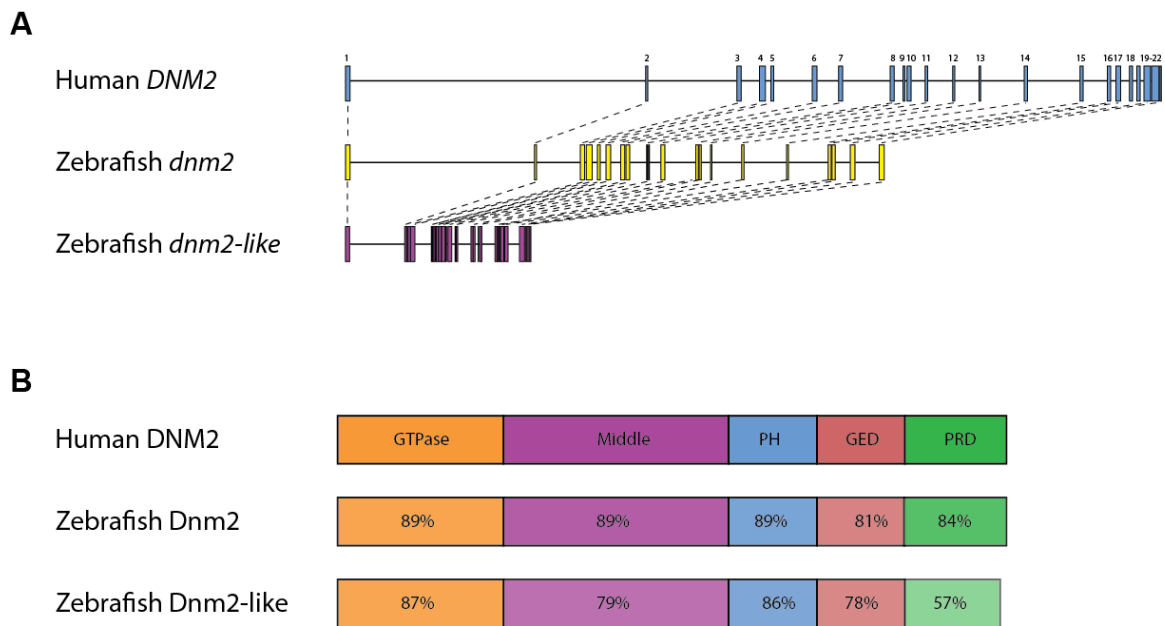


Figure 2-2: Molecular and protein structure of *dnm2* and *dnm2-like*

(A) Intron-exon organization of human *DNM2*, zebrafish *dnm2* and zebrafish *dnm2-like*. (B) Protein structure of zebrafish Dnm2 and Dnm2-like compared to human DNM2. Percent identity between zebrafish and human protein domains was calculated by BLASTP (PH, pleckstrin homology domain; GED, GTPase effector domain; PRD, proline-rich domain).

2.3.2 *dnm2* and *dnm2-like* genes are widely expressed in adult and embryonic tissue

To determine the expression pattern of *dnm2* and *dnm2-like*, we performed RT-PCR on adult zebrafish tissues and whole zebrafish larvae from several time points. Both *dnm2* and *dnm2-like* mRNA was detected in all adult tissues examined (Figure 2-3, A). Both genes products were also detected at the earliest stages of development, indicating that both *dnm2* and *dnm2-like* are likely maternally deposited mRNAs (Figure 2-3, B).

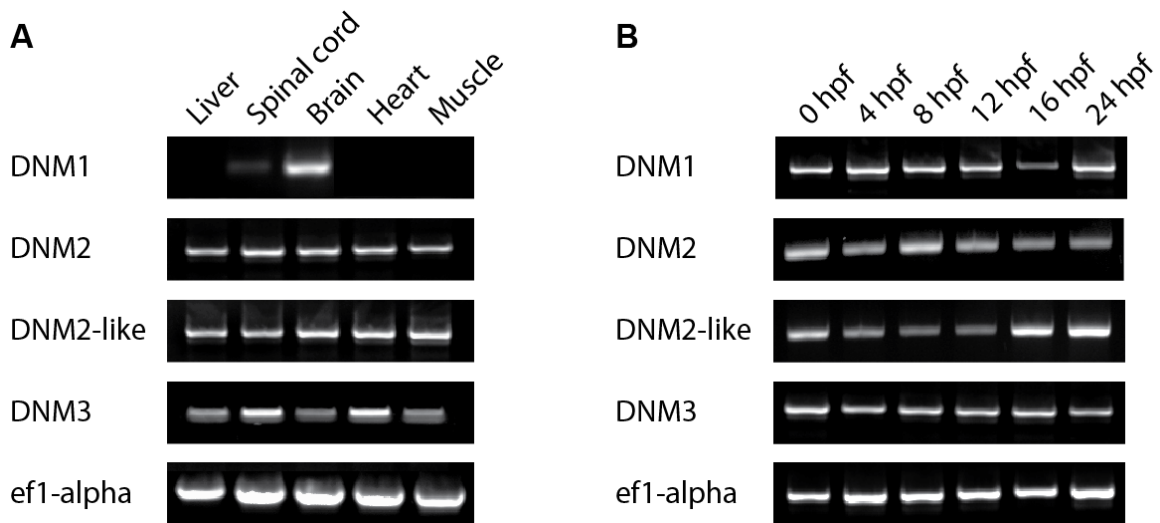


Figure 2-3: Spatial and temporal expression of *dnm2* and *dnm2-like*

(A) RT-PCR was used to assay expression levels of *dnm2* and *dnm2-like* in tissues isolated from adult zebrafish. Primers for *ef1 α* were used as an internal control. (B) RT-PCR was used to assay expression levels of *dnm2* and *dnm2-like* between 0 hours post fertilization (hpf) and 24 hpf. All classical dynamins appear to be deposited as maternal mRNAs and expressed throughout early development.

2.3.3 Morpholino-mediated knockdown of zebrafish dynamin-2 gene expression

To better clarify the roles of *dnm2* and *dnm2-like*, we used targeted morpholino oligonucleotides to knockdown expression of both genes during early development. Morpholinos were targeted to splice junctions in unprocessed *dnm2* and *dnm2-like* mRNAs, and the resulting products were confirmed to be out of frame by sequencing the RT-PCR products (Figure 2-4). A standard control morpholino was injected for comparison (Gene-Tools).

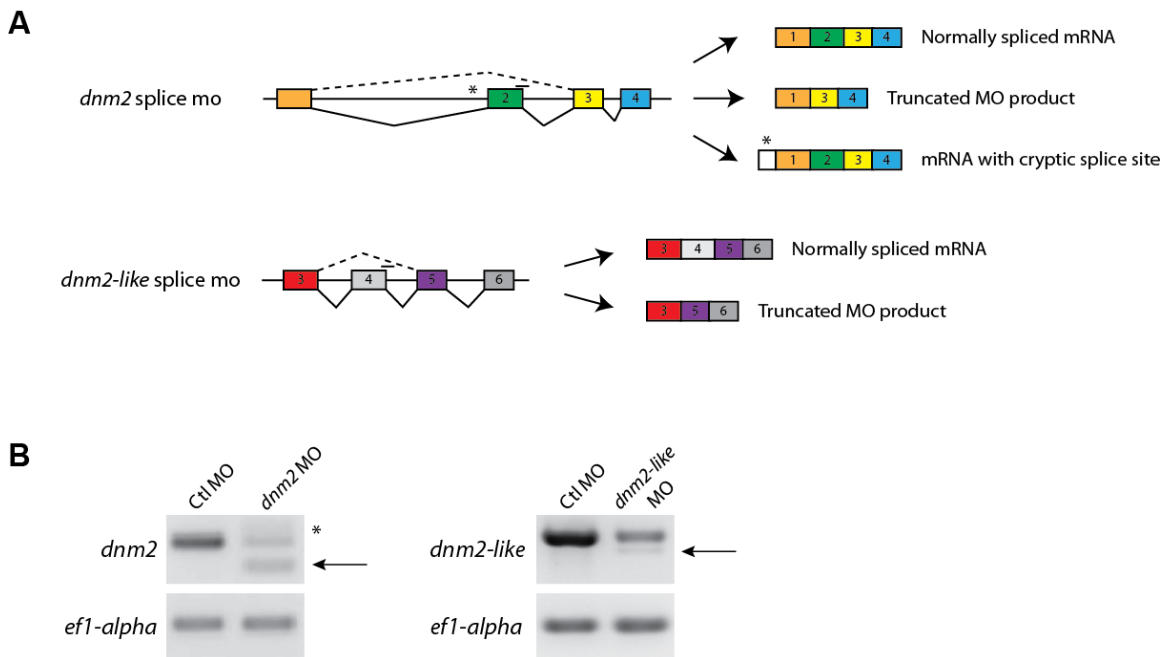


Figure 2-4: Morpholino-mediated knockdown of *dnm2* and *dnm2-like*

(A) Splice targeting morpholinos were designed against intron-exon boundaries within the *dnm2* and *dnm2-like* genes. (B) Knockdown in morpholino injected embryos was verified using RT-PCR. Control embryos were injected with a scrambled control morpholino (Ctl). Arrows indicate the alternative splice product induced by morpholino injection. The *dnm2* morpholino resulted in an additional higher weight band due to activation of a cryptic splice site (asterisk).

Both morpholinos resulted in pronounced but non-overlapping developmental phenotypes (Figure 2-5, A-C). Knockdown of DNM2 caused a shortened body axis, small eyes, yolk and cardiac edema, shortened somites and an upward tail curvature. Knockdown of DNM2-like resulted in a thinned body axis, small eyes, and pigmentation defects. The severity and penetrance of morpholino phenotypes was consistent between injections. At 48 hpf, 93% of *dnm2* morphants and 74% of *dnm2-like* morphants exhibited the described phenotypes (Figure 2-5, D; control $n=601$, *dnm2* $n=598$, *dnm2-like* $n=587$; data combined from 9 trials). 4% of control embryos displayed developmental abnormalities unrelated to the morphant phenotypes.

To examine dynamin-2 protein expression in *dnm2* and *dnm2-like* morphants, isolated muscle fibers were stained with an antibody against rat dynamin-2. Cells from both *dnm2* and *dnm2-like* morphants had reduced staining relative to control morphants.

2.3.4 Expression of human DNM2 rescues *dnm2* and *dnm2-like* knockdown

To rescue the *dnm2* and *dnm2-like* morphant phenotypes, embryos were co-injected with human DNM2 capped mRNA and morpholino at the 1- to 2-cell stage. Expression of DNM2 RNA did not cause any abnormalities in control-injected embryos. At 48 hpf, the percent of normal-appearing embryos was significantly increased in both rescue conditions. In *dnm2* morphants, the percent of normal embryos increased from 8.2% to 67.1% ($p<0.0001$, Fisher's exact test). In *dnm2-like* morphants, the percent of normal embryos increased from 24.2% to 45.8% ($p<0.0001$, Fisher's exact test). These data suggest that the morphant phenotypes were not due to off-target effects of the MOs.

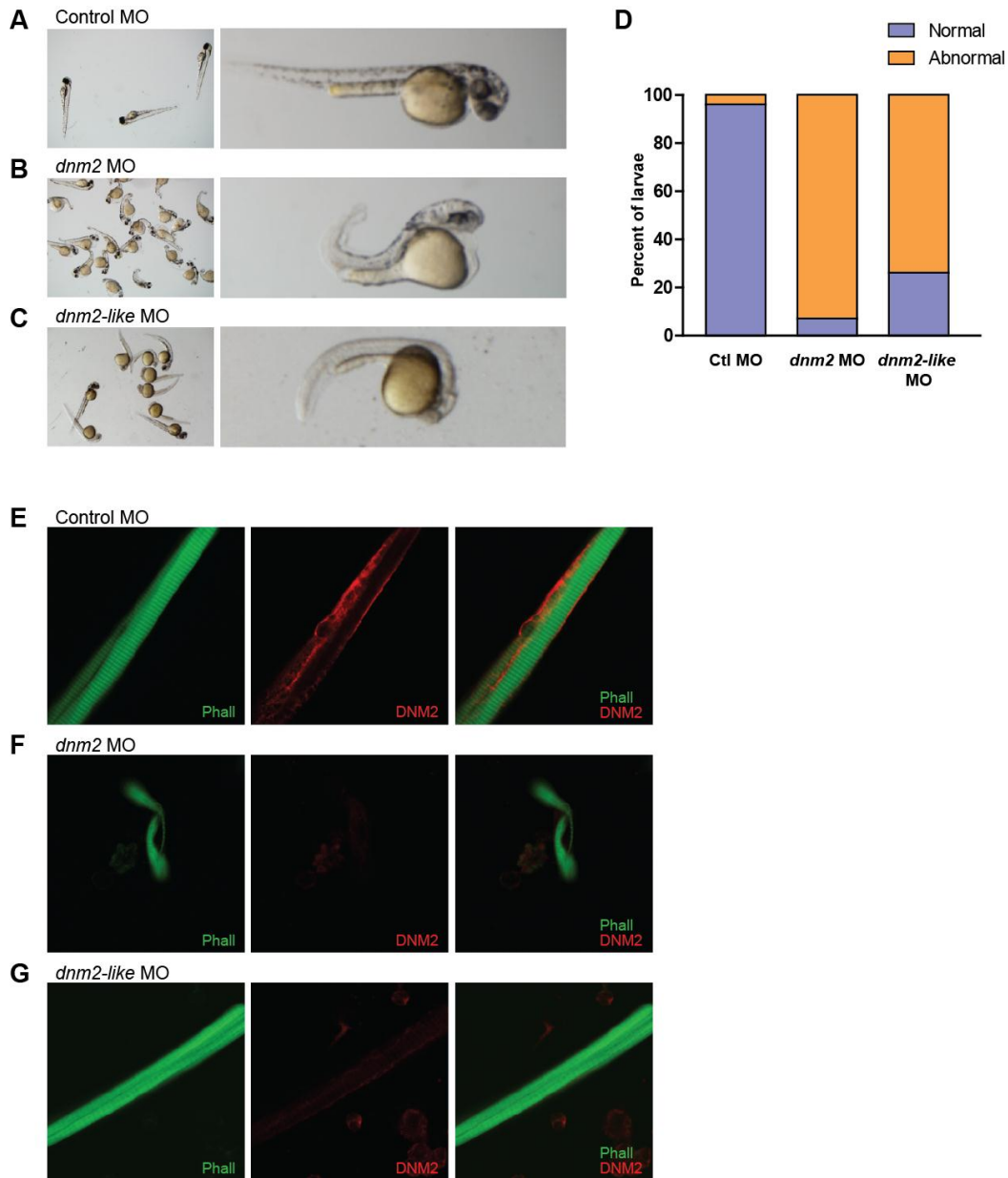


Figure 2-5: Knockdown of *dnm2* and *dnm2-like* results in morphological changes

(A-C) *dnm2* and *dnm2-like* morphants at 48 hours. Standard control morpholino (A) was injected for comparison. (B) At 48 hpf, *dnm2* morpholino injected embryos exhibit shortened body length, upward curled tails, pericardial and yolk edema, and reduced head size when compared to control morpholino injected embryos. By contrast, embryos injected with *dnm2-like* morpholino (C) have small muscle compartments, pigmentation defects, and mild tail curvature. (D) Percent of affected embryos at 48 hpf (control $n=601$, *dnm2* $n=598$, *dnm2-like* $n=587$; data combined from 9 trials). (E-G) Dynamin-2 staining in muscle fibers from morpholino-injected larvae at 3 dpf.

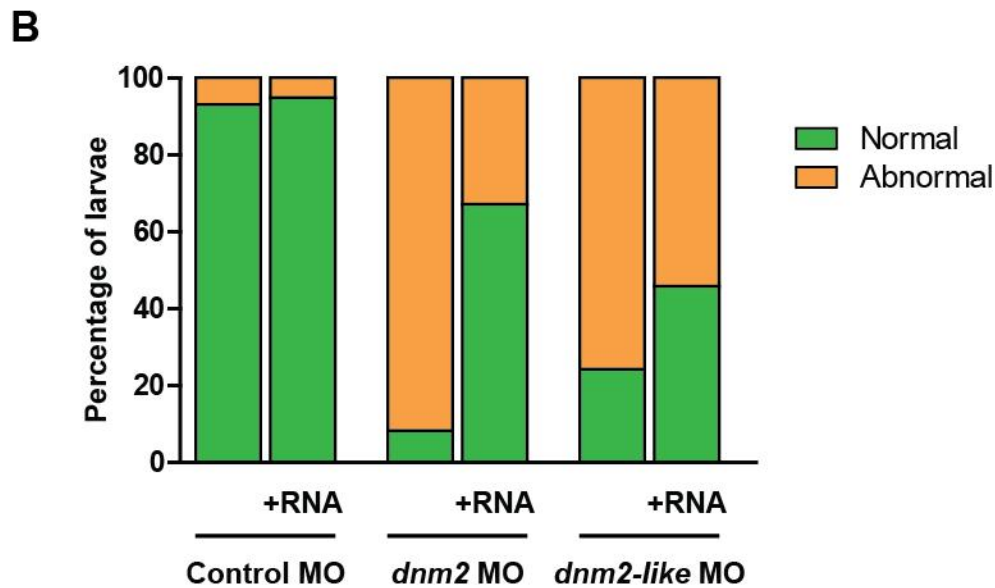
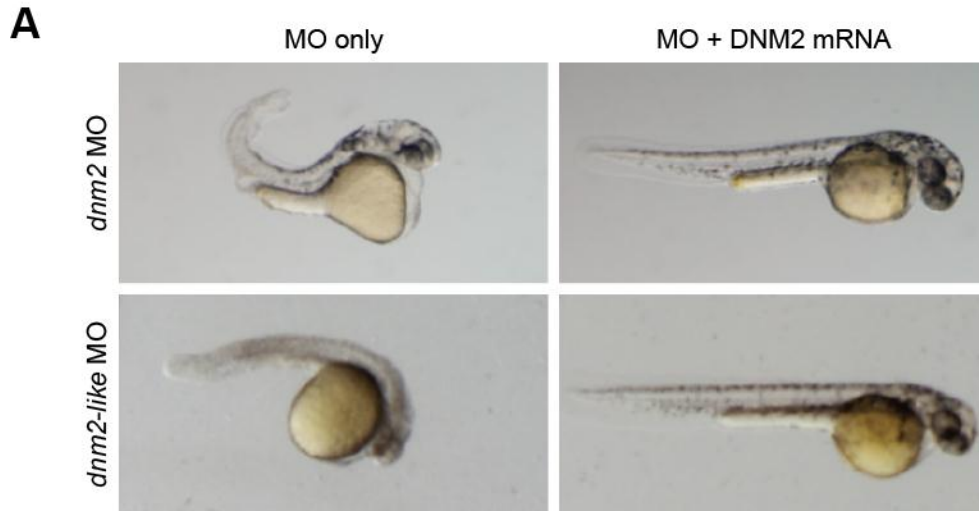


Figure 2-6: Human DNM2 RNA rescues *dnm2* and *dnm2-like* morphant phenotypes

Rescue of *dnm2* and *dnm2-like* morphants at 48 hpf. (A) Co-injection of human DNM2 RNA can rescue morphological abnormalities in both morphants. (B) The percentage of normal appearing larvae is significantly increased in both *dnm2* and *dnm2-like* rescue conditions (control $n=407$, *dnm2* $n=397$, *dnm2-like* $n=418$; *dnm2* $p<0.0001$, *dnm2-like* $p<0.0001$, Fisher's exact test).

2.4 Discussion

In this study, we identify two dynamin-2 genes in the zebrafish genome. The two genes are likely a product of the whole genome duplication that occurred in the ray fin fish lineage prior to the evolution of the teleost [91, 92]. The syntenic organization of both genes supports this conclusion. *dnm2* (zebrafish chromosome 3) shares close syntenic conservation with *DNM2* (human chromosome 19), as it is directly flanked by homologs of the upstream and downstream neighbors of human *DNM2* (*TMED1* and *QTRT1*). While *dnm2-like* (zebrafish chromosome 1) does not share this immediate syntenic block, the human homologs of at least four nearby genes are found within a .5 Mb distance of human *DNM2* (*CDC37*, *LPAR2*, *CDC37* and *RDH8*). Additionally, both zebrafish genes are found near chromosomal regions that have previously been reported to share homology with human chromosome 19 [93].

At both the gene and protein level, *dnm2* and *dnm2-like* share structural similarity with human *DNM2*. All three genes have a similar intron-exon organization, although *dnm2-like* has much smaller introns. Shrinkage of introns has been reported in several other teleost homologs to human genes [94-96]. At the protein level, the predicted amino acid sequences of Dnm2 and Dnm2-like share a high percent identity to human *DNM2*, as well as to each other. When we examined the DNA sequence of other human and zebrafish classical dynamins, phylogenetic analysis sequence grouped *dnm2* and *dnm2-like* with *DNM2* rather than *DNM1* or *DNM3*.

Mammalian *DNM2* is ubiquitously expressed in adult tissue [12-14]. In zebrafish, we found *dnm2* and *dnm2-like* expression in every tissue we examined, which suggests these genes may also be ubiquitously expressed. Both genes were also expressed

throughout early development. The early presence of these gene products makes it likely that *dnm2* and *dnm2-like* mRNAs are maternally deposited.

In this study we observe developmental abnormalities following knockdown of either *dnm2* or *dnm2-like*. It is important to note that both morpholino reagents used in this chapter are splice-targeting morpholinos, which only target unprocessed mRNA transcripts. Therefore, expression of maternally deposited mRNAs will not be knocked down by morpholino oligonucleotides. Since we detect *dnm2* and *dnm2-like* mRNA at the one-cell stage, it is likely that both genes products are unaffected by morpholino knockdown during the first few hours of development. In spite of this, we see distinct morphological defects in both *dnm2* and *dnm2-like* morphants by 24 hpf. Expression of human *DNM2* can partially rescue both phenotypes, which supports the hypothesis that *dnm2* and *dnm2-like* share functional homology with human *DNM2*.

Taken together, our findings show that *dnm2* and *dnm2-like* are highly conserved orthologs to human *DNM2*. It will be important to further examine these two genes in order to understand their specific cellular function in the zebrafish. The zebrafish provides an excellent system for examining aspects of membrane trafficking *in vivo*, and understanding the zebrafish dynamin-2 homologs will allow a more precise analysis of these pathways.

2.5 Materials and Methods

Animal care: Zebrafish (AB strain) were bred and raised according to established protocols, under the guidelines of the University of Michigan Animal Care and Use protocols. Experiments were performed on zebrafish embryos and larvae between 1 and 2 dpf. All animals were handled in strict accordance with good animal practice as defined by national and local animal welfare bodies. All animal work was approved by the University of Michigan Committee for the Use and Care of Animals (UCUCA protocol #09835).

Phylogenetic and syntenic analysis: Multiple species alignments and phylogenetic analysis were performed using Mega 5.1 software. Phylogenies were created using the neighbor-joining method with 1000 bootstrap replicates. Syntenic genes were identified using NCBI and Ensembl databases, and orthology of these genes was confirmed using reciprocal BLAST searches against the human and zebrafish genomes.

RACE-PCR and RT-PCR: Rapid amplification of cDNA end (RACE) was performed to confirm the 3' sequence of zebrafish *dnm2*, using the 3'-RACE GeneRacer kit (Invitrogen) according to the manufacturer's protocol. To clone *dnm2*, total RNA was extracted from 48 hpf larvae using the RNeasy kit (Qiagen). For expression studies, RNA was extracted from adult tissue zebrafish tissue and embryos at various developmental timepoints. For analysis of morpholino-mediated knockdown, RNA was extracted from injected larvae at 48 hpf. cDNA was synthesized from RNA using the iScript cDNA Synthesis kit (Bio-Rad). PCR was performed on a MyCycler thermocycler (BioRad) using GoTaq Green 2x Master Mix (Promega) and primers to zebrafish *EFl-alpha*, *dnm2*, and *dnm2-like*.

RNA synthesis: Wild-type human DNMT2 plasmid was purchased from Invitrogen (ORF Gateway® Entry IOH53617). Expression vectors were generated by recombination of DNMT2 entry clones with p5E-CMV/SP6, p3E-polyA, and pDestTol2pA2 cassettes from the Tol2kit v1.2, a kind gift of Dr. Chi-Bin Chien [97]. Gateway recombination reactions were performed using LR Clonase II Plus Enzyme Mix (Invitrogen). The DNMT2 rescue plasmid was linearized with NotI and transcribed using the SP6 mMessage Machine kit (Ambion).

Morpholino and RNA injection of zebrafish embryos: For *dnmt2* and *dnmt2-like* knockdown, the following splice targeting morpholinos were designed:

5'-TGCCGTGCTCATTAACACACTCACC-3' (*dnmt2*)

5'-CAACCCCACTGCTCTCACCGGATCT-3' (*dnmt2-like*).

Custom morpholinos, along with standard control morpholino, were purchased from Gene Tools. Fertilized eggs were collected after timed matings of adult zebrafish and injected at the 1–2-cell stage using a Nanoject II injector (Drummond Scientific).

Embryos were injected with a .1 mM (*dnmt2-like*) or .3 mM (*dnmt2*) concentration, in a 4.6 nL volume. For rescue experiments, embryos were co-injected with human DNMT2 RNA at a 30 ng/μl concentration. Larvae were photographed using a Nikon AZ-100 microscope or a *Leica MXIII Stereoscope*.

Myofiber Cultures: Mixed cell cultures from 72 hpf embryos were isolated as previously described [74]. Briefly, larvae were dissociated in 10 mM collagenase type I (Sigma) for 60–90 min at room temperature. Embryos were triturated every 30 min. Dissociated preps were pelleted by centrifugation, resuspended in CO₂ independent

media (Invitrogen), passed through a 70 mm filter (Falcon), and plated onto chamber slides (Falcon) precoated with poly-L-Lysine (Sigma). After 4 hours, cells were fixed for 15 min in 4% paraformaldehyde

Statistical analysis: Statistical analysis was performed on data using the GraphPad Prism 5 software package. Significance was determined using Fisher's exact test.

Chapter 3: Neuromuscular junction abnormalities in DNM2-related CNM

3.1 Abstract

Dynamamin-2 related centronuclear myopathy (DNM2-CNM) is a clinically heterogeneous muscle disorder characterized by muscle weakness and centralized nuclei on biopsy. There is little known about the muscle dysfunction underlying this disorder, and there are currently no treatments. In this study, we establish a novel zebrafish model for DNM2-CNM by transiently overexpressing a mutant version of DNM2 (DNM2-S619L) during development. We show that overexpression of DNM2-S619L leads to pathological changes in muscle and a severe motor phenotype. We further demonstrate that the muscle weakness seen in these animals can be significantly alleviated by treatment with an acetylcholinesterase inhibitor. Based on these results, we retrospectively analyzed the clinical history of two patients with DNM2-CNM and found evidence suggesting abnormal neuromuscular transmission. Together, our results suggest that deficits at the neuromuscular junction may play an important role in the pathogenesis of DNM2-CNM and that treatments targeting this dysfunction can provide an effective therapy for patients with this disorder.

3.2 Introduction

Centronuclear myopathies (CNMs) are a clinically heterogeneous group of muscle disorders characterized by a high proportion of centralized nuclei on muscle biopsy. CNMs can have a wide spectrum of clinical presentations, ranging from severe infantile to mild adult-onset forms. Common features of the disease include generalized weakness, poor muscle tone, ptosis, and ophthalmoparesis. Mutations in four genes are known to cause CNM: myotubularin (*MTM1*), amphiphysin 2 (*BINI*), dynamin 2 (*DNM2*), and the skeletal muscle ryanodine receptor (*RYR1*).

To date, 14 different mutations in *DNM2* have been shown to cause autosomal dominant forms of CNM (Figure 3-1, A). While the relationship between mutation location and phenotype is not entirely clear, patients with severe early-onset *DNM2*-CNM often have mutations in the pleckstrin homology (PH) domain. The PH domain is responsible for localizing *DNM2* to the plasma membrane during endocytosis, but this localization does not seem to be disrupted by disease-associated mutations in the PH domain [68, 71]. At the plasma membrane, *DNM2* forms rings around budding vesicles, where it contributes to the release of newly-formed endosomes. In addition to endocytic function, *DNM2* has been implicated in caveolae internalization, trans-Golgi transport, and aspects of cytoskeletal regulation including lamellipodial extension, phagocytosis, cell motility, cell division, and centrosome cohesion [3, 6, 98-102].

Despite the well-characterized role of *DNM2* in endocytosis, little is known about *DNM2* function in muscle or the specific pathomechanisms that underlie *DNM2*-related CNM. The purpose of this study is to examine the structure and function of the neuromuscular junction (NMJ) in *DNM2*-CNM using a novel zebrafish model and

retrospective analysis of patients with DNM2-CNM. While NMJ defects have not typically been associated with CNM pathology, some patients with CNM exhibit symptoms consistent with congenital myasthenic syndromes, a group of disorders caused by defects in neuromuscular transmission. Case studies have reported NMJ abnormalities in patients with genetically uncharacterized CNM, including histopathologic features that resemble the post-synaptic changes seen in some myasthenic disorders [77, 79, 80]. Intriguingly, two recent studies describe patients with CNM who responded favorably to treatment with acetylcholinesterase inhibitors, a finding consistent with NMJ deficits [82, 83]. Despite this mounting evidence that CNM can present with myasthenic features, there are no reports of NMJ dysfunction or acetylcholinesterase inhibitor treatment in patients with DNM2-CNM.

There are currently no transgenic DNM2-CNM animal models that recapitulate the major features of the disorder. Heterozygous knock-in mice carrying the R465W mutation display some histologic changes and modest muscle atrophy by 8 months, but exhibit no overt motor phenotype or centralized nuclei [85]. By contrast, viral overexpression of DNM2-R465W in adult mouse muscle causes weakness and muscle atrophy, and a significant increase in abnormally localized nuclei by four weeks post-injection [84]. Both of these mouse studies examined the DNM2-R465W mutation, a common CNM-causing mutation. Most patients with the DNM2-R463W mutation have a relatively mild disease course, with symptom onset ranging from late childhood to the 4th decade of life [35, 44]. In this study, we examine transient overexpression of DNM2-S619L, a mutation associated with severe neonatal weakness and hypotonia [103].

Zebrafish have been a successful model for many muscle disorders, and our lab has previously characterized a zebrafish model for myotubular myopathy, an X-linked form of CNM [63, 74]. In this study, we generate a novel model of DNM2-CNM by transiently overexpressing DNM2-S619L in developing zebrafish larvae. These animals exhibit severe weakness and motor deficits. We demonstrate that NMJs are disorganized in these animals, and that motor dysfunction can be rapidly alleviated by acetylcholinesterase inhibitor treatment. We also show electrophysiological evidence for NMJ deficits in two patients with DNM2-CNM, and report symptomatic improvement following acetylcholinesterase inhibitor treatment. Taken together, these results suggest that deficits in neuromuscular transmission are a significant component of DNM2-CNM pathology, and that therapeutics targeting the NMJ may provide effective treatment for this disorder.

3.3 Results

3.3.1 Motor behavior is impaired in DNM2-S619L injected embryos

To examine the effect of DNM2-S619L overexpression in zebrafish, embryos were injected with DNM2-WT or DNM2-S619L capped mRNA at the 1- to 2-cell stage. Two RNA concentrations were tested, 50pg per injection and 150pg per injection. Reverse-transcriptase PCR was performed on RNA extracted from injected embryos at 1 day post fertilization (dpf), 2 dpf and 3 dpf. Although levels of injected DNM2 RNA decreased over time, RNA was still present at 3 dpf (Figure 3-1, D). Injections with either construct did not cause an obvious defect in general body morphology (Figure 3-1, B). Since injections at the lower concentration of RNA resulted in a pronounced motor phenotype, all measurements were performed on larvae injected with 50pg of RNA.

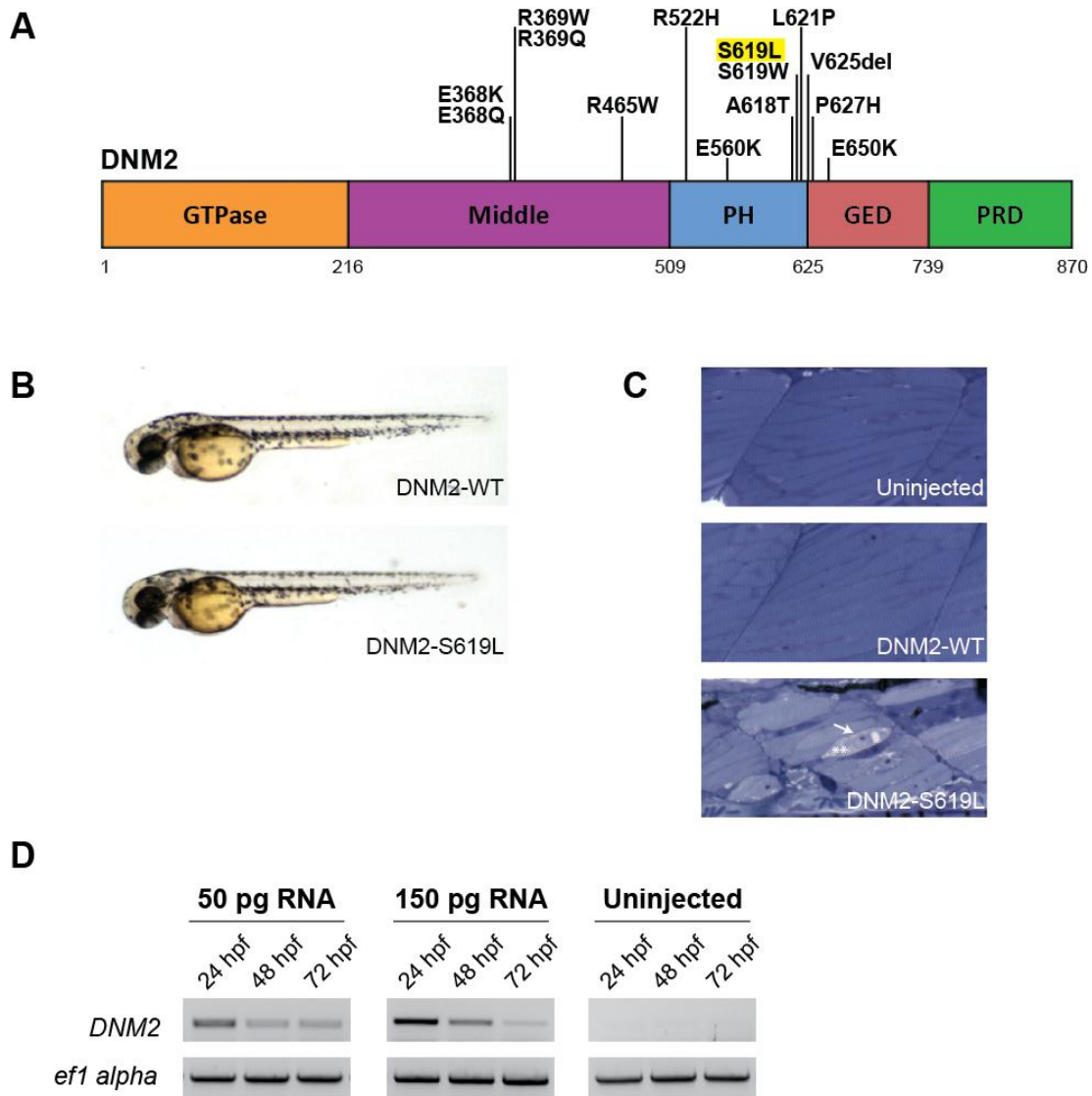


Figure 3-1: Overexpression of DNM2-S619L causes a muscle-specific phenotype

(A) CNM-causing mutations in human DNM2. The mutation used in this study, DNM2-S619L, is highlighted in yellow. (B) DNM2-WT and DNM2-S619L larvae at 2 dpf. Overexpression of DNM2-WT or DNM2-S619L does not cause any gross morphological changes during development. (C) Semi-thin sections of DNM2-WT and DNM2-S619L muscle at 3 dpf. Note large internal nuclei (arrow) with disorganized perinuclear material (**) in DNM2-S619L muscle. (D) RT-PCR of human DNM2 expression in developing zebrafish injected with high (150 pg/injection) or low (50 pg/injection) concentrations of DNM2-S619L RNA. All further studies were performed on embryos injected with 50 pg RNA.

At 2 dpf, larvae expressing DNM2-S619L had notably weaker swimming patterns and frequently exhibited a weak “flutter” tail movement. When lightly tapped, most DNM2-S619L larvae were unable to generate a substantial escape response (Figure 3-2, A). To further quantitate this phenotype, we examined the escape response at 3 dpf. 35% of DNM2-S619 larvae failed to respond to tactile stimulus, compared with 13% of DNM2-WT larvae and 5% of uninjected larvae (Figure 3-2, B; uninjected $n=401$, DNM2-WT $n=386$, DNM2-S619L $n=398$; data combined from 10 trials). In addition to non-responsive larvae, many DNM2-S619L larvae responded to touch with a light tail flutter or body coil, but did not swim away from the stimulus. 39% of DNM2-S619 larvae responded with a flutter or coil, compared with 12% of DNM2-WT larvae and 1% of uninjected larvae. Animals that were able to swim away from the stimulus (regardless of speed) were included in the “swim” category. 94% of uninjected and 74% of DNM2-WT larvae were able to swim away from the stimulus, while only 26% of DNM2-S619L larvae responded by swimming.

3.3.2 Histopathological abnormalities in DNMS2-S619L zebrafish

To determine if there were structural abnormalities within skeletal muscle that associated with the impaired motor function, semi-thin sections from injected control, DNM2-WT and DNM2-S619L embryos (2 dpf) were analyzed ($n = 3$ per condition). As compared to control muscle, no overt histopathologic changes were observed in the DNM2-WT muscle. Conversely, abundant abnormalities were observed in the muscle from DNM2-S619L embryos. These changes included large, unusually shaped and positioned nuclei (black arrow in Figure 3-1, C), the presence of disorganized, amorphous cellular material in the perinuclear area (** in Figure 3-1, C), and additional

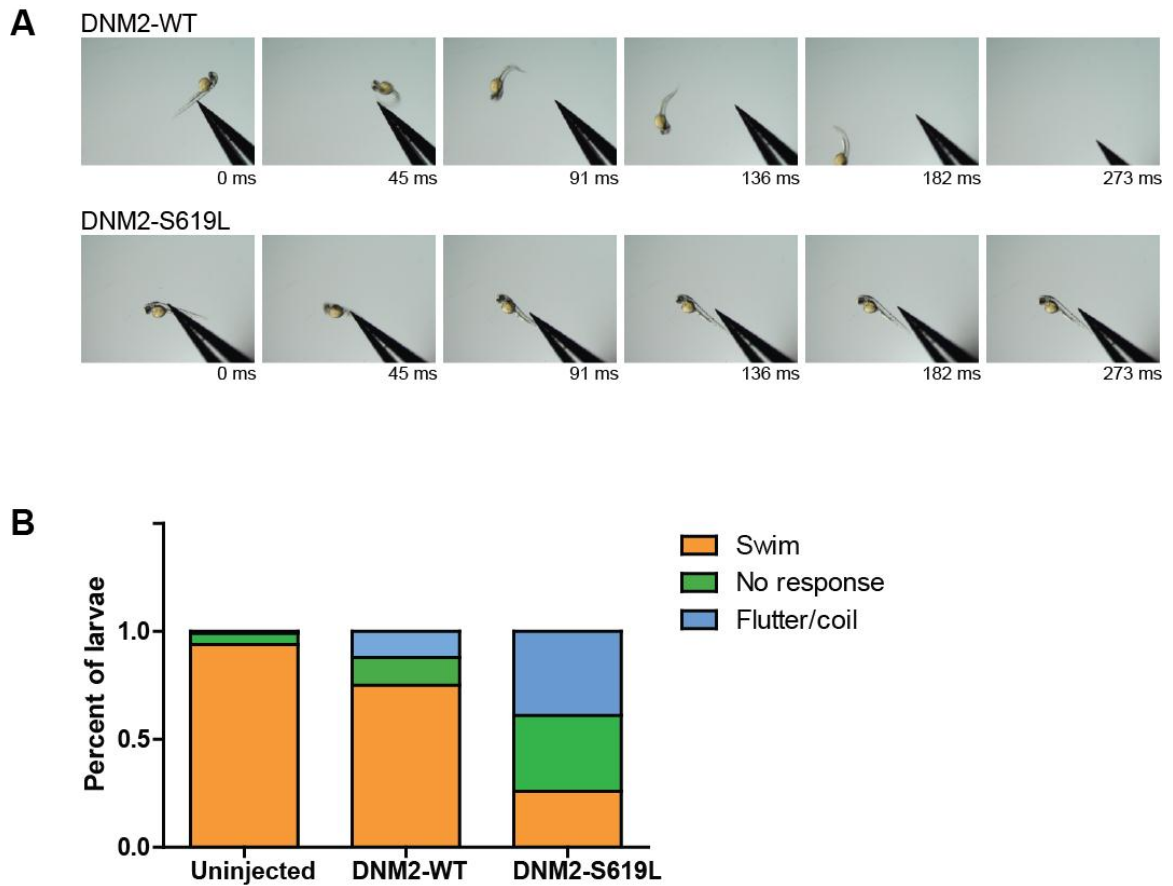


Figure 3-2: DNM2-S619L larvae exhibit impaired motor function

(A) Video frames showing tail tap stimulus of a DNM2-WT larva (above) and a DNM2-S619L larva (below). (B) Response to tail tap stimulus at 3 dpf (uninjected $n=401$ larvae, DNM2-WT $n=386$, DNM2-S619L $n=398$, response scores combined from 10 different trials).

areas of swollen intracellular organelles (white arrow). The overall muscle compartment was also smaller than controls, implying that muscle fiber size was smaller. Taken together, these changes are consistent with those reported for other models of CNM in zebrafish and are in keeping with the predicted features of a centronuclear myopathy [74].

To examine the organization of the developing NMJs, we used alpha-bungarotoxin to stain for acetylcholine receptor clusters (Figure 3-3). In 3 dpf DNM2-S619L larvae, the clusters are weaker and more dispersed, although the general distribution appears normal and they localized with motor axon path. This attenuated staining was seen in 18 of 21 DNM2-S619L larvae, and not observed in DNM2-WT larvae ($n=19$).

3.3.3 Acetylcholinesterase inhibitor treatment improves motor behavior in zebrafish

To further examine the role of the NMJ in the observed motor defects, we measured the response of DNM2-S619L and DNM2-WT larvae to treatment with edrophonium, a short-acting acetylcholinesterase inhibitor. Short treatments with 0.2 mg/mL edrophonium (1-5 minutes) dramatically increased both spontaneous and evoked movement in DNM2-S619L larvae. Following treatment, DNM2-S619L larvae that had previously exhibited little or no movement were able to swim away from a tail tap stimulus (Figure 3-4, A).

To quantify the improvement seen in acetylcholinesterase inhibitor-treated DNM2-S619L larvae, we measured the distance swum in approximately 182 ms following a tail tap stimulus (Figure 3-3,B; $n=10$ for all conditions). Only larvae that exhibited a motor response prior to treatment were included. In the measured time interval, uninjected larvae swam an average distance of 53.8 ± 4.5 mm. Before treatment, DNM2-WT larvae swam 46.9 ± 3.0 mm, and DNM2-S619L larvae swam 21.4 ± 4.9 mm. The distance swum by the DNM2-S619L larvae was significantly smaller than the uninjected or DNM2-WT groups ($P < 0.001$). Following acetylcholinesterase

inhibitor treatment, the DNM2-S619L larvae swam significantly further than before treatment ($P < 0.01$). There was no significant difference between the distance swum by the treated DNM2-S619L group as compared to DNM2-WT larvae or to uninjected controls. Of note, neither DNM2-WT nor uninjected control larvae had a change in swim behavior following acetylcholinesterase inhibitor treatment.

To further examine the response to acetylcholinesterase inhibitor treatment, DNM2-S619L larvae were embedded in agarose with the tail and caudal portion of the fish free to move (Figure 3-4, C). All larvae exhibited weak and restricted tail beats during swim bouts ($n=6$). Following 2 minutes of acetylcholinesterase inhibitor treatment, all larvae moved with increased tail curvature and stronger muscle contractions (Figure 3-4, C).

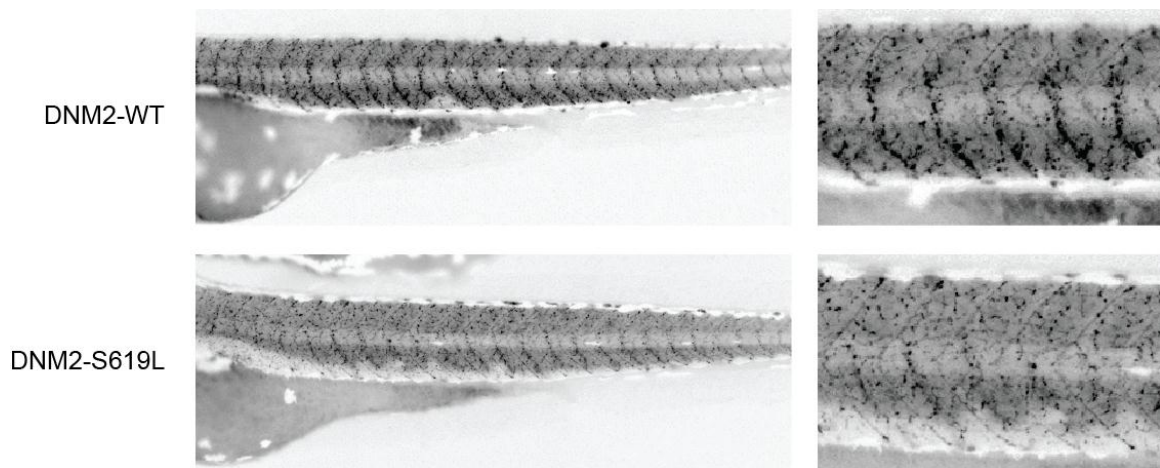


Figure 3-3: Acetylcholine receptor distribution is disrupted in DNM2-S619L larvae

At 3 dpf, DNM2-WT larvae exhibit normal acetylcholine receptor clustering (above). DNM2-S619L larvae exhibit fewer puncta along the motor axon path (below).

The maximum tail extension of each larva was measured before and after treatment, and was found to increase in all treated larvae (Figure 3-4, D). Prior to acetylcholinesterase inhibitor treatment, DNM2-S619L larvae had an average maximum tail extension of 14.2% of body length. Following treatment, the average maximum tail extension was 51.8% of body length ($p > 0.0005$).

3.3.4 Abnormal NMJ function and response to acetylcholinesterase inhibitor in two individuals with DNM2-related CNM

To understand the potential relevance of these findings in zebrafish to human DNM2-related CNM, two cases histories were retrospectively analyzed.

Case 1: Case 1 is a 24 year old male individual. He presented with weakness and respiratory failure shortly after birth, and he has been wheelchair and ventilator dependent for his entire life. In addition to severe extremity weakness, he also has ptosis, ophthalmoparesis, and lower facial weakness. Muscle biopsy performed in the first year of life was consistent with a diagnosis of centronuclear myopathy (significantly increased central nuclei, abnormal oxidative stain pattern, and type I fiber predominance and atrophy). Genetic testing was negative for mutations in *MTM1* but revealed a heterozygous mutation (S619L) in *DNM2*.

This individual had a relatively static course of illness until approximately 1 year ago. In the past year he has experienced progressive fatigue as well as declining strength that is manifested by decreased volume of speech and diminished ability to raise his distal upper extremity against gravity. Clinical evaluation did not reveal any general medical condition to account for his decline, and his cardiorespiratory status (include nocturnal ventilatory status) was unchanged. Electrodiagnostic studies were performed,

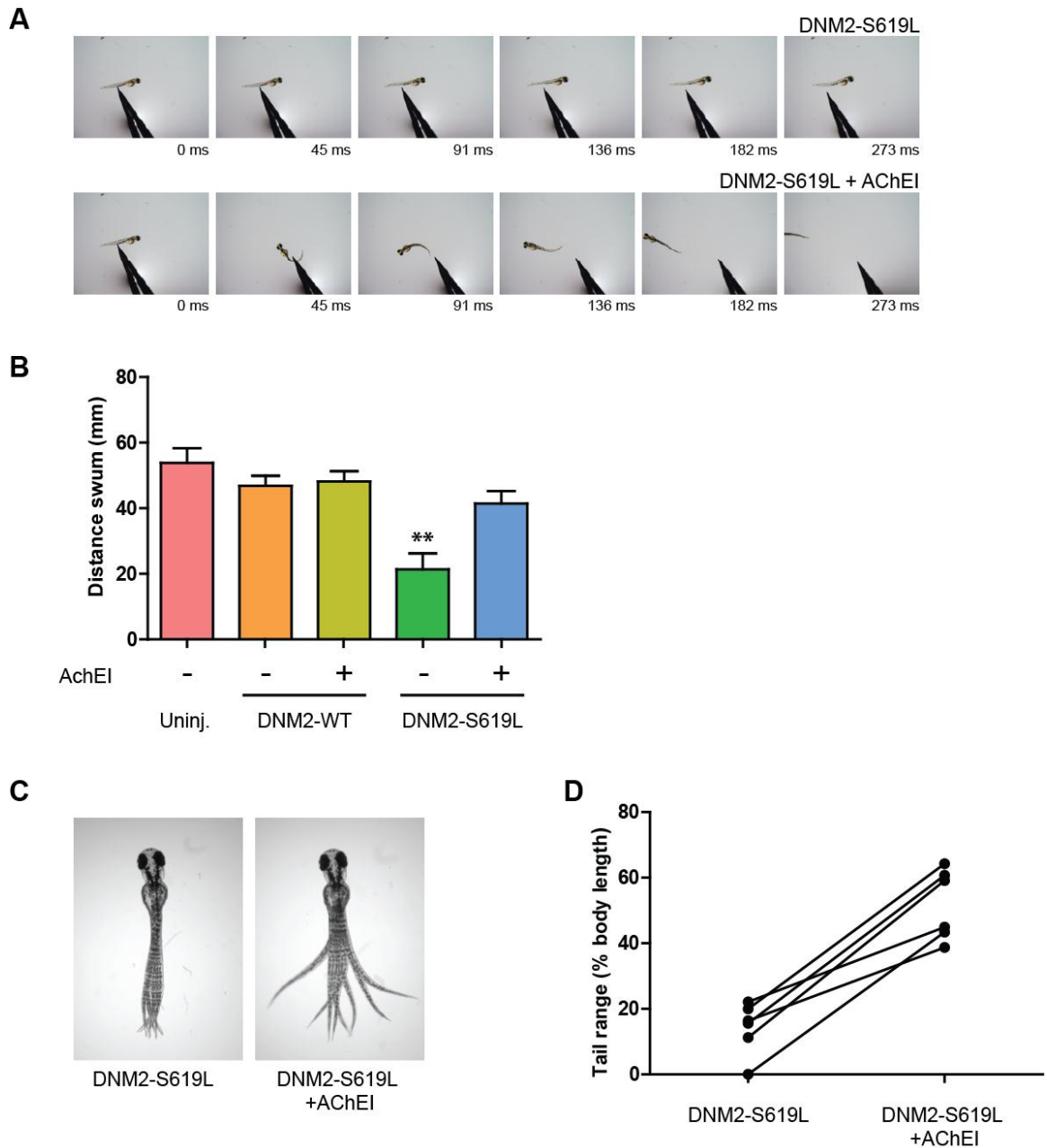


Figure 3-4: AChEI treatment improves motor behavior in DNM2-S619L larvae.

(A) Touch evoked response in a 3 dpf larva. Tail tap prior to treatment (above) and following 2 minute acetylcholinesterase inhibitor (AChEI) treatment (below, same animal). (B) Average swim distances within 180ms, with and without AChEI treatment ($p < 0.01$ one-way ANOVA, Tukey post-hoc test). (C) Agarose embedded larvae at 3 dpf, video frame composite over 340ms. Swim bursts prior to treatment (left) and following 2 minute AChEI treatment (right, same animal). (D) Maximum tail extension of individual DNM2-S619L larvae, with and without AChEI treatment.

including 3 Hz repetitive nerve stimulation and single fiber electromyography (SFEMG). A 6 to 12% decrement was observed with 2 Hz repetitive stimulation of the ulnar motor compound muscle action potential . SFEMG of the right Extensor Digitorum Brevis revealed neuromuscular jitter (a measure of neuromuscular transmission synchrony between two motor units) in all motor unit pairs with a mean consecutive difference (MCD) from 88 to 300 μ sec (normal 25 to 35 μ sec) with several motor unit pairs having > 20% blocking, an indication of complete loss of neuromuscular synchrony. Based on these findings, he was started on pyridostigmine therapy at a dose of 60mg QID. Within 2 weeks of treatment, he reported improvement in several areas. Specifically, his speech was higher in volume and easier to understand, he had less complaints of fatigue, and, for the first time since early childhood, he was able to bring his hands to his mouth. He has been continued on this dose of pyridostigmine and has maintained these improvements in motor function. Of note, acetylcholine receptor antibody testing was negative.

Case 2: Case 2 is a 28 year old female who began to experience weakness around 5 years of age. Her presenting symptoms were frequent falls and an abnormal gait with difficulties rising from a seated position and climbing stairs. A diagnostic muscle biopsy performed at age 8 revealed changes consistent with centronuclear myopathy (excessive central nuclei, small type I fibers, and a spoke-on-wheel appearance with NADH staining). Genetic testing uncovered a heterozygous mutation (E368K) in DNMT2. The basic clinical details of this patient have been reported previously [38].

She has had progressive decline in motor function, has additionally developed severe ptosis and ophthalmoparesis, and has for the past 3 years required a cane for

ambulation and for the past year has required a walker. She has also experienced worsening fatigue and exercise intolerance, and at her worst was able to take only a few steps with a walker before needing to stop. Based on this increasing fatigue and declining motor function, she underwent an electrodiagnostic evaluation. Two Hz repetitive stimulation of the ulnar motor and spinal accessory motor compound action potentials were normal with no decrement. SFEMG of the triceps revealed neuromuscular jitter with a MCD of 40 μ sec (normal 25 to 35 μ sec). She was subsequently started on pyridostigmine therapy at a dose of 60 mg QID. She reported subjective improvement with medication, stating she had much more energy and improved ambulation with her walker. Her dose of medication was reduced to 30 mg QID due to excessive diarrhea, and on this dose she continues to claim having increased exercise tolerance and diminished fatigue. Of note, her acetylcholinesterase antibody test was negative.

3.4 Discussion

In this study, we demonstrate motor weakness and NMJ defects in a novel zebrafish model of DNM2-CNM. Larval fish overexpressing human DNM2-S619L have disorganized acetylcholine receptor patterning and severe motor deficits manifested in weak tail beats, slow swimming, and partial paralysis. We show that motor dysfunction in these animals can be rapidly alleviated by treatment with an acetylcholinesterase inhibitor. Additionally, we report clinical and electrophysiological findings consistent with NMJ deficits in two patients with DNM2-CNM. Each patient responded favorably to acetylcholinesterase inhibitor therapy, providing further evidence for a defect in neuromuscular transmission in DNM2-related CNM.

This study provides the first evidence of a NMJ defect in *DNM2*-related CNM. There are several previous reports of abnormal histologic findings in NMJs from patients with genetically unconfirmed CNM that support the relevance of our findings. At least three studies have described abnormal endplate elongation and irregular acetylcholinesterase staining [77-79], and one ultrastructural study reported post-synaptic junctional folds that were irregular and unelaborated [80]. Two recent studies provide clinical evidence for NMJ involvement in some CNM patients. Liewluck et al. described a patient with genetically uncharacterized CNM combined with clinical, histological, and electrophysiological features of myasthenia [82]. Similarly, Robb et al. reported three patients with genetically uncharacterized CNM and one patient with a mutation in *MTM1* who exhibited fatigability and abnormal jitter on EMG [83]. All four patients responded favorably to acetylcholinesterase inhibitor treatment, and two patients showed substantial improvement with sustained therapy. In this same report, our lab demonstrated that a zebrafish model of myotubular myopathy has abnormal acetylcholine receptor patterning and that motor weakness in these animals can be partially alleviated by acetylcholinesterase inhibitor treatment. These case reports on myotubular myopathy and unconfirmed CNM thus corroborate our findings in *DNM2*-CNM.

Our data, when considered with these previous studies, supports a growing body of evidence that NMJ defects are a clinical feature of many, if not all, subtypes of CNM. Neuromuscular transmission deficits have now been identified in two genetically defined subsets of CNM, those associated with mutations in *MTM1* and *DNM2*. Together with previous reports of NMJ abnormalities in genetically uncharacterized patients, these findings underscore the importance of examining NMJ function in all CNM patient

populations. While further study is needed to determine the prevalence of neuromuscular transmission deficits, it is possible that they are a common feature among all or most patients with CNM. Since this aspect of the disease is therapeutically tractable, this opens up new avenues for the treatment of CNM.

In addition, our work suggests that DNM2 may directly participate in the establishment or regulation of the NMJ. Nothing is known about the function of DNM2 at the post-synaptic NMJ; however, several factors make it an excellent candidate to consider in the regulation of the post-synaptic NMJ. DNM2 is well characterized as a membrane trafficking protein and it plays a role in shaping and remodeling a variety of membrane structures in most cell types. In addition to functioning in membrane deformation, DNM2 associates with many components of the cytoskeleton, which is required for stabilization of NMJ post-synaptic components [104, 105]. At neuronal synapses, DNM2 has also been shown to interact with scaffolding proteins that shape the post-synaptic density during development [106]. In light of the evidence presented here, it will be important for future studies to examine the specific function of DNM2 at the NMJ.

In summary, we have shown that transient expression of DNM2-S619L in zebrafish is a novel model for DNM2-CNM. We have identified a new mechanism of disease based on this model, which is supported by clinical evidence from two patients with mutations in DNM2. These results suggest that NMJ deficits are a significant component of DNM2-CNM pathology, and that acetylcholinesterase inhibitors can be an effective therapy for patients with this disorder. Our findings further show that zebrafish

are an excellent model for DNM2-CNM and can provide important insight into the pathomechanisms of DNM2-CNM and related disorders.

3.5 Materials and Methods

Animal care: Zebrafish (AB strain) were bred and raised according to established protocols, under the guidelines of the University of Michigan Animal Care and Use protocols. Experiments were performed on zebrafish embryos and larvae between 1 and 3 dpf. All animals were handled in strict accordance with good animal practice as defined by national and local animal welfare bodies. All animal work was approved by the University of Michigan Committee for the Use and Care of Animals (UCUCA protocol #09835).

RNA synthesis and injection of zebrafish embryos: Wild-type human DNM2 plasmid was purchased from Invitrogen (ORF Gateway® Entry IOH53617). The S619L point mutation was introduced using the QuikChange Lightning Site-directed Mutagenesis kit (Stratagene). Expression vectors were generated by recombination of DNM2 entry clones with p5E-CMV/SP6, p3E-polyA, and pDestTol2pA2 cassettes from the Tol2kit v1.2, a kind gift of Dr. Chi-Bin Chien [97]. Gateway recombination reactions were performed using LR Clonase II Plus Enzyme Mix (Invitrogen). DNM2 expression constructs were linearized with NotI and transcribed using the SP6 mMessage Machine kit (Ambion). Fertilized eggs were collected after timed matings of adult zebrafish and injected at the 1–2-cell stage using a Nanoject II injector (Drummond Scientific). Embryos were injected with 50 pg or 150 pg of RNA (10.9 ng/uL or 32.6 ng/uL in an injection volume of 4.6 nL) and raised in E2 embryo culture media [107].

Analysis of motor behavior: Larvae were photographed using a Nikon AZ-100 microscope or a Leica MXIII Stereoscope. For tail movement studies, larvae were embedded in 1% low melting point agarose and agarose surrounding the tail was gently cut away. Tail extension measurements were performed using ImageJ (NIH) and calculated as percent of body length. For acetylcholine esterase inhibitor studies, zebrafish larvae were bathed in 0.2 mg/mL edrophonium (Enlon®, Bioniche Pharmaceuticals) diluted in E2 media. Touch-evoked motor behaviors were elicited by touching the tail with a pair of No. 5 forceps. Speed measurements and video frame capture were performed using ImageJ (NIH).

Reverse transcription PCR: RNA was isolated from embryos at 1, 2, or 3 dpf using the RNeasy kit (Qiagen). cDNA was synthesized from RNA using the iScript cDNA Synthesis kit (Bio-Rad). PCR was performed on a MyCycler thermocycler (BioRad) using GoTaq Green 2x Master Mix (Promega) and primers to zebrafish EF1-alpha or human DNM2.

Histopathologic analysis: For semi-thin sections, zebrafish were fixed overnight in Karnovsky's fixative at 3 dpf and then processed for embedding in epon by the Microscopy and Imaging Laboratory core facility at the University of Michigan. Semi-thin sections were stained with toluidine blue and photographed using an Olympus BX43 microscope. For fluorescent imaging, acetylcholine receptors were labeled with Alexa Fluor 594 conjugated alpha-bungarotoxin (Invitrogen, 1:100 in PBST) and photographed using a Nikon Microphot FXA microscope.

Statistical analysis: Statistical analysis was performed on data using the GraphPad Prism 5 software package. Where relevant, significance was determined using a one-way ANOVA, followed by Tukey's multiple comparison test. For maximum tail extension measurements, a paired Student's t-test was used to determine significance.

Case studies: Retrospective case data was collected via institutional review board (IRB approved protocols (HUM00032624 and HUM00030880) at the University of Michigan.

Chapter 4: Alterations in excitation-contraction coupling in DNM2-related CNM

4.1 Abstract

Transverse tubules (t-tubules) and sarcoplasmic reticulum (SR) are specialized organelles that mediate excitation-contraction coupling in skeletal muscle. Recent evidence suggests that t-tubule and/or SR defects may contribute to disease pathology in some forms of centronuclear myopathy, a group of muscle disorders characterized by muscle weakness and centralized nuclei on biopsy. Mutations in the dynamin-2 gene (*DNM2*) cause an autosomal dominant form of centronuclear myopathy (DNM2-CNM). In this study, we examined the relationship between DNM2 and the structure of the sarcotubular network. We observed motor function defects and abnormalities in muscle structure in *dnm2*-deficient zebrafish larvae. We also looked at histopathological changes in muscle from a transient zebrafish model of DNM2-CNM. Both of these models exhibited substantial disorganization of the sarcotubular network. Spontaneous calcium release was also decreased in muscle from DNM2-S619L fish. We additionally found that DNM2-S619L expression alters tubule patterning in a cellular *ex vivo* model of t-tubule formation. This suggests that DNM2 functions in either the formation or maintenance of these structures, and that CNM-associated mutations can alter this function. Taken together, these data support a role for DNM2 in sarcotubular membrane architecture.

4.2 Introduction

Efficient muscle contraction is dependent on highly ordered membrane components of the myofiber. The two main membrane structures are transverse tubules (t-tubules) and the sarcoplasmic reticulum (SR). T-tubules are deep invaginations of the plasma membrane, which conduct electrical excitation into the interior of the cell. T-tubules are closely aligned with the SR, a network of specialized endoplasmic reticulum containing large stores of calcium. The interaction between t-tubules and SR is responsible for excitation-contraction (EC) coupling, the translation of an electrical stimulus into a muscle contraction. When an action potential is propagated across the myofiber, voltage-sensitive proteins in the t-tubule trigger the release of calcium from the SR. Together, these two organelles mediate downstream muscle contraction and relaxation through the rapid release and uptake of calcium.

Recent evidence suggests that t-tubule and/or SR defects may contribute to muscle dysfunction in centronuclear myopathy (CNM), a genetically and clinically heterogeneous group of muscle disorders. Currently, mutations in four genes are known to cause CNM: *MTM1*, *DNM2*, *BIN1* and *RYR1*. In three different animal models of myotubular myopathy, ultrastructural analysis has revealed abnormal organization of the triad, the specialized junction where a t-tubule aligns with the terminal cisternae of the SR [74-76]. Similar findings were reported in a viral overexpression model of DNM2-CNM [84]. In patients with CNM, a number of studies have reported mislocalization of triad markers on biopsies from patients with MTM1-CNM, DNM2-CNM or BIN1-CNM [53, 57, 74].

Together, these histopathologic findings point to a potential shared mechanism of disease in different genetic subsets of CNM. However, while it has been suggested that CNM-linked genes might act together in establishing or maintaining muscle organelles, a common pathway has yet to be established. Furthermore, only two of these genes encode proteins with a known role at the t-tubule or SR: *RYR1*, which encodes the skeletal ryanodine receptor (an SR calcium channel found in complex with voltage-sensitive proteins of the t-tubule) and *BINI*, which encodes amphiphysin 2 (a protein involved in t-tubule biogenesis) [72, 73]. Nothing is currently known about the role of DNM2 or MTM1 in t-tubule or SR function, although both proteins have important functions in membrane trafficking.

In order to better understand the relationship between DNM2 and the sarcotubular network, we examined muscle from two zebrafish models established in our lab. First, we looked at motor function and muscle histology in larval zebrafish with reduced *dnm2* expression (*dnm2* morphants). Second, we examined muscle histology in a transient model of DNM2-CNM (DNM2-S619L larvae). In both models, we see substantial disorganization of the sarcotubular membrane network. In support of these findings, we show that expression of mutant DNM2 substantially alters tubule organization in a cellular *ex vivo* model of t-tubule formation. We further demonstrate that calcium release, the functional output of the SR, is substantially decreased in DNM2-S619L fish. Together, this evidence provides strong support for the hypothesis that DNM2 is required for maintaining normal organization of the sarcotubular network in muscle, and that this function is specifically disrupted by a CNM-linked mutation in DNM2.

4.3 Results

4.3.1 Knockdown of zebrafish *dnm2* homolog disrupts motor behavior

As described in Chapter 2, we previously identified two zebrafish homologs to human DNM2. In addition to the morphological changes described in Chapter 2, we found that knocking down expression of *dnm2* (chromosome 3) resulted in a pronounced motor phenotype. During early development, few fish exhibited spontaneous or evoked motor activity. At 24 hpf, spontaneous coiling was significantly reduced in *dnm2* morphants (Figure 4-1, A; $p < 0.0001$, control $n = 135$, *dnm2* $n = 137$, data combined from 4 trials). Control morphant embryos contracted an average of 35.1 ± 1.4 times per minute, while *dnm2* morphant embryos contracted 11.9 ± 1.1 . At 48 hpf, most *dnm2* morphant fish did not respond to a tail tap stimulus (Figure 4-1, C-D). 74% of *dnm2* morphants did not swim in response to a tail tap, as compared with 3% of control injected larvae and 1% of uninjected larvae.

4.3.2 Knockdown of *dnm2* alters membrane structures of the contractile apparatus

To understand the specific effect of *dnm2* knockdown on muscle organization, we examined ultrastructural changes using electron microscopy. At 3 dpf, control larvae had well-ordered muscle fibers aligned with the SR and t-tubules (Figure 4-2, A, C). The t-tubules and SR met at regular intervals to form triads (Figure 4-2, E, G, I). By contrast, we found substantial disorganization of t-tubules and SR in *dnm2* morphants (Figure 4-2, B, D). Although the muscle retained the typical sarcomere striations seen in control larvae, there was notable accumulation of excess membrane. While there were some

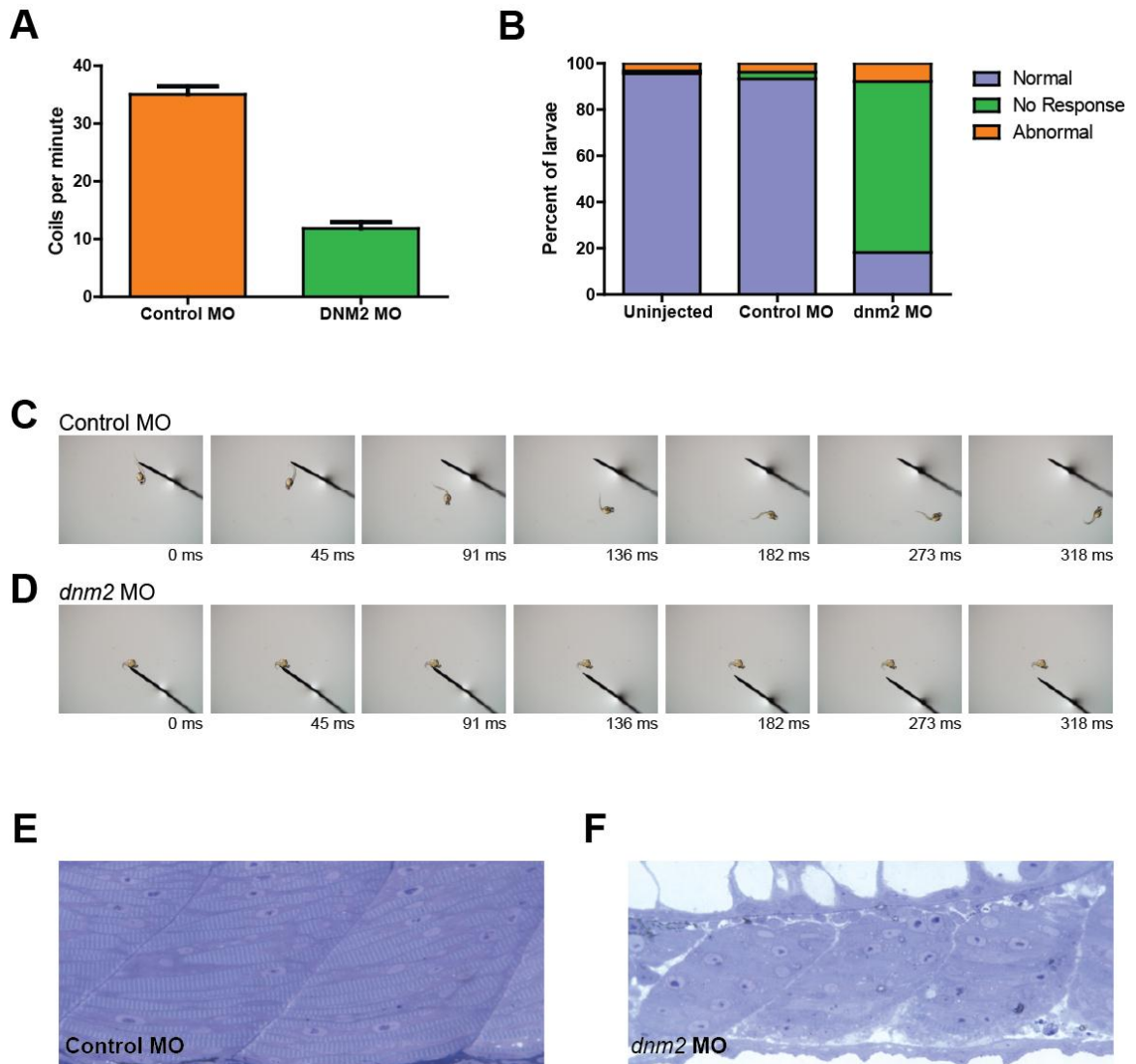


Figure 4-1: Motor deficits and muscle disorganization in *dnm2* knockdown fish.

(A-B) Knockdown of *dnm2* alters motor behavior in developing zebrafish. (A) At 24 hpf, the rate of spontaneous coiling in zebrafish embryos is significantly decreased. (B) At 48 hpf, most zebrafish larvae fail to respond to tail tap stimulus. (C-D) Video frames showing tail tap stimulus of a control morphant and a *dnm2* morphant. (E-F) Semithin sections of muscle from 72 hpf control or *dnm2* morpholino injected larvae.

normal triad structures present in morphant muscle (Figure 4-2, C), most provided striking examples of triad disorganization (Figure 4-2, F, H, J). Specifically, we noted the frequent absence of a defined t-tubule or terminal cisternae, as well as an excess of membrane in the longitudinal regions of the SR. We also noted regions of perinuclear disorganization in morphant larval muscle, as compared with controls (Figure 4-2, A, B).

4.3.3 DHPR localization in *dnm2* morphant muscle fibers

In light of the ultrastructural changes observed in *dnm2* knockdown muscle, we examined t-tubule organization by immunohistochemistry. Isolated muscle fibers were prepared from 3 dpf larvae injected with control or *dnm2* morpholino. Muscle fibers were then stained using an antibody against DHPR, a receptor localized to the t-tubule. Immunofluorescence revealed that DHPR appeared to appropriately localize in ordered striations along the myofiber in both control and *dnm2* morphant larvae (Figure 4-3, A-B). However, there was also extra accumulation of DHPR along the sarcolemma. To better examine the distribution of DHPR staining, three dimensional reconstructions were generated from confocal Z-stack images of cells. The rendering of a *dnm2* morphant fiber revealed short, distended t-tubules as compared to the t-tubules in the control fiber (Figure 4-3, C-D).

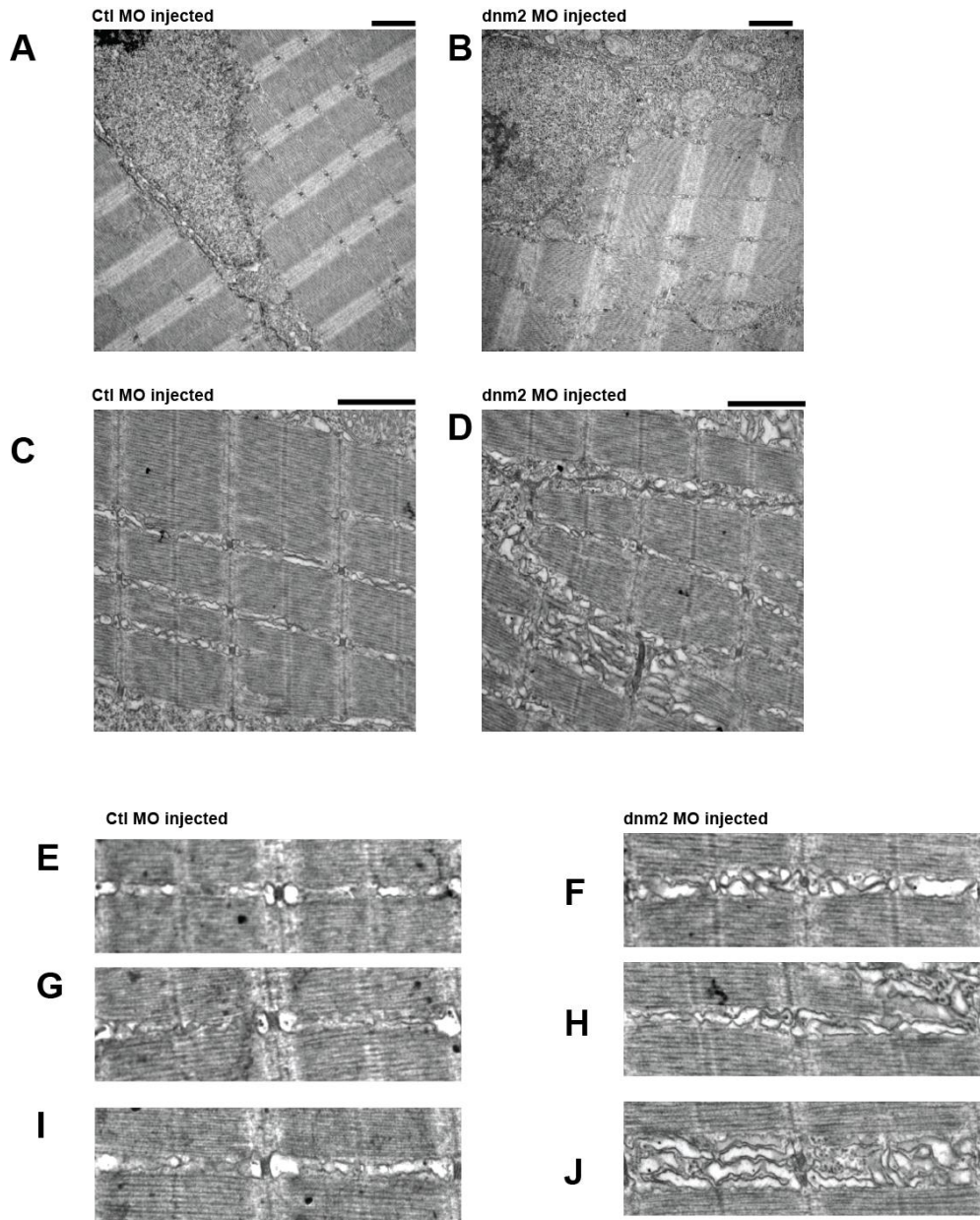


Figure 4-2: *dnm2* knockdown disrupts membrane structure in muscle fibers.

Electron micrographs of longitudinal sections through zebrafish muscle. (A,B) Abnormal perinuclear accumulations were present in some regions of *dnm2* knockdown muscle. (C,D) Although muscle from *dnm2* knockdown larvae retains general organization, there is a notable accumulation of membranous structures. While some normal triads were present in *dnm2* muscle (F), there were many triads with abnormal organization (H, J). Scale bar equal to 1 micron.

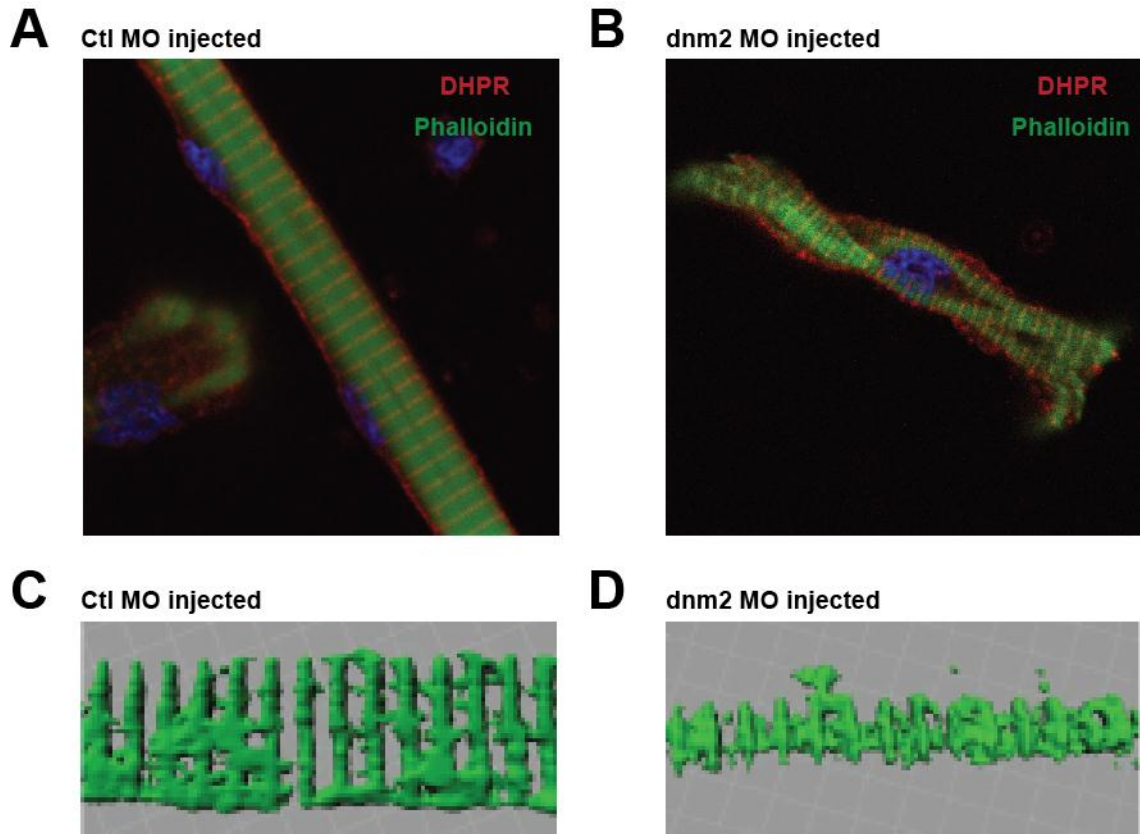


Figure 4-3: Effects of DNM2 knockdown on DHPR localization.

(A-B) DHPR staining in isolated fibers from control and *dnm2* morphants at 3 dpf. DHPR is localized to developing t-tubules in both conditions. (C-D) Three dimensional rendering of DHPR staining reveals short and distorted membrane organization in *dnm2* morphant fibers.

4.3.4 DNM2-S619L expression alters formation of BIN1-induced tubules

Since knockdown of *dnm2* altered t-tubule and SR organization in zebrafish muscle, we wanted to examine the effect of a CNM-associated mutation on the organization of these organelles. To this end, we generated constructs containing human DNM2 with the S619L mutation, a CNM-causing mutation associated with severe neonatal weakness and hypotonia [103]. To determine if the S619L mutation could alter membrane organization, we examined DNM2-S619L overexpression in an *ex vivo* model of tubulation. Overexpression of amphiphysin-2 in non-muscle cells induces the formation of tubular membrane structures, which has previously been used to model t-tubule biogenesis [53, 72]. Using *cos7* cells, we co-expressed GFP-tagged amphiphysin 2 (BIN1 isoform 8, a kind gift of Pietro De Camilli) with mCherry-tagged wild type DNM2 (DNM2-WT) or DNM2 with an S619L mutation (DNM2-S619L). Consistent with previous results, we found that co-expression of BIN1 and DNM2-WT resulted in extensive tubulation in *cos7* cells. However, when DNM2-S619L was co-expressed with BIN1, we saw the formation of short punctate structures instead of tubules. Tubulation in each cell was classified as short, long or intermediate (DNM2-WT $n=68$, DNM2-S619L $n=73$, cells from three independent experiments).

4.3.5 Muscle membrane structures are altered in DNM2-S619L larval muscle

Electron micrographs of DNM2-WT and DNM2-S619L muscle were obtained at 3 dpf. We identified substantial membrane abnormalities in the muscle of DNM2-S619L (Figure 4-5, B, D, F). Although there were some regions with normal-appearing t-tubules and SR, there were also expansive regions with swollen SR, disorganized t-tubules and expanded vacuole-like structures. We also noted regions with high numbers of mitochondria as compared to DNM2-WT larvae (Figure 4-5, A-B).

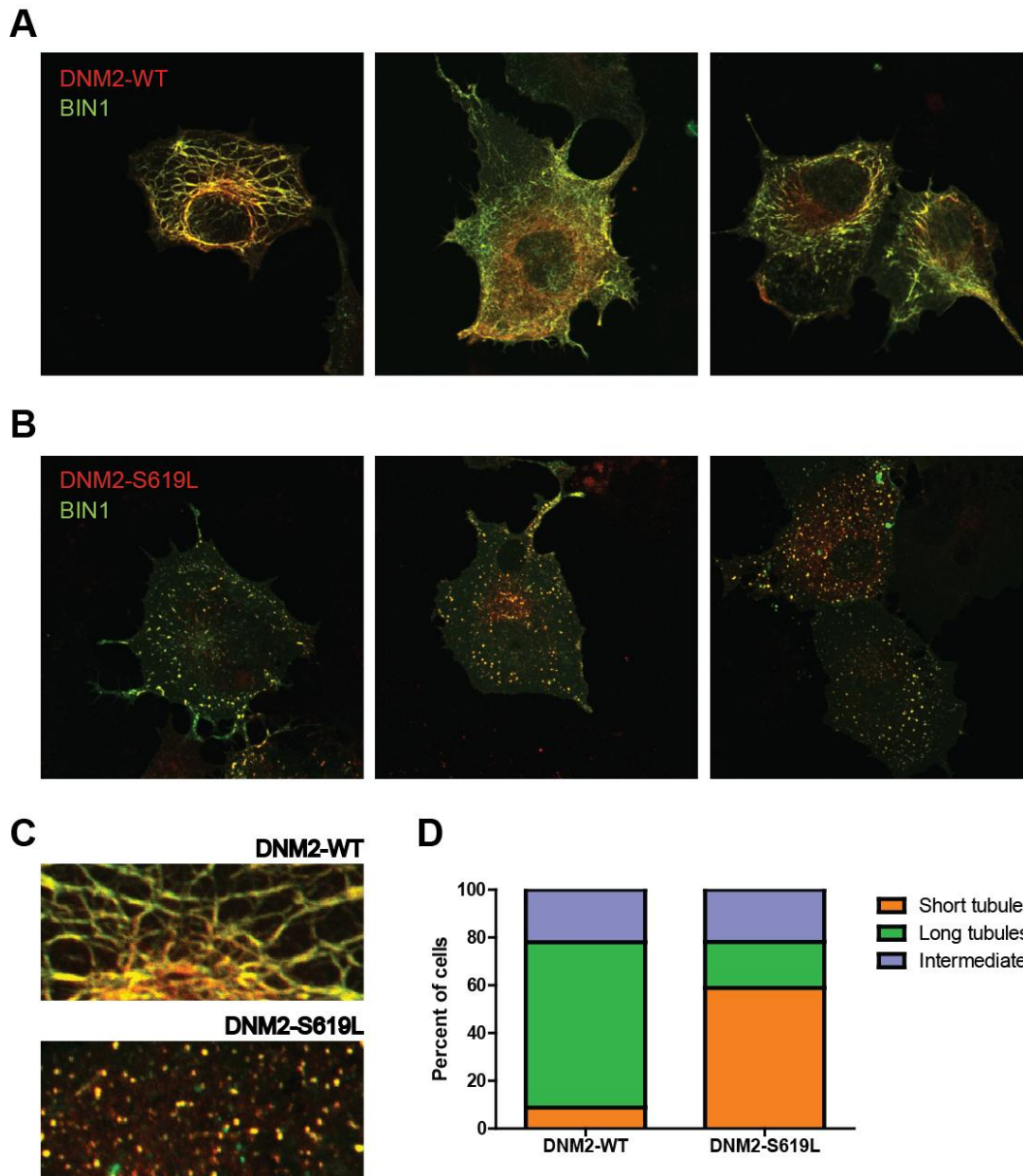


Figure 4-4: DNM2-S619L expression alters *ex vivo* tubulation in COS cells.

(A) Co-expression of mCherry DNM2-WT and GFP BIN1. DNM2 and BIN1 co-localize to a complex membranous network of tubules induced by BIN1-overexpression. (B) Co-expression of BIN1 with DNM2-S619L disrupts the normal distribution of these networks. (C) Quantification of tubulation in BIN1-induced cells overexpressing DNM2-WT vs. DNM2-S619L. While 69% of DNM2-WT expressing cells exhibit long tubules, only 19% of DNM2-S619L expressing cells have a long tubule phenotype (DNM2-WT $n=68$, DNM2-S619L $n=73$, data combined from 3 independent experiments.)

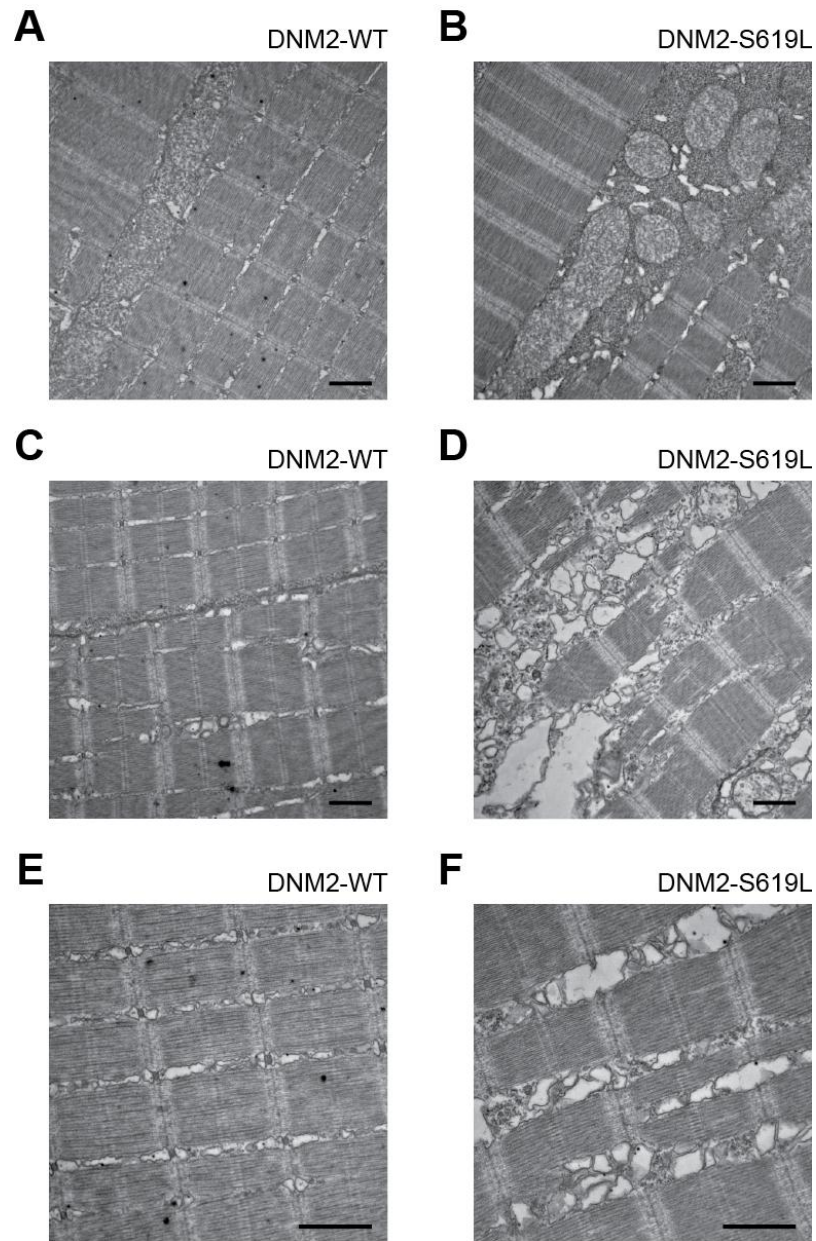


Figure 4-5: T-tubule and SR abnormalities in DNM2-S619L larval muscle.

Electron micrographs of longitudinal sections through zebrafish muscle at 3 dpf. (A, C, E) Muscle from DNM2-WT larvae shows the typical sarcomere striations of vertebrate striated muscle. (B, D, F) Muscle from DNM2-S619L larvae. There is extensive swelling and vacuolization in the region of the SR and t-tubules. Scale bar equal to 1 micron.

4.3.6 Reduced calcium flux in the muscle of DNM2-S619L larvae

In order to examine the functional effect of DNM2-S619L expression on EC coupling, we examined calcium transients in spontaneously contracting embryos using a genetically encoded calcium indicator. Embryos were co-injected with 50 pg of DNM2 RNA and 100 pg of gCaMP DNA at the 1-2 cell stage, and screened for variegated gCaMP expression in skeletal muscle (Figure 4-6, A). Both DNM2-WT and DNM2-S619L larvae expressed gCaMP at a similar level. At 24 hours, embryos were embedded in agarose and fluorescence was measured during spontaneous muscle contractions. Although all embryos examined displayed muscle contractions with normal timing, the DNM2-S619L embryos exhibited almost no visible increase in fluorescence during muscle contractions (Figure 4-6, C-D; DNM2-WT $n=6$, DNM2-S619L $n=6$; representative data shown). In order to directly compare fluorescence between embryos, $\Delta F/F$ was calculated for fluorescent recordings of muscle contractions (Figure 4-5, B).

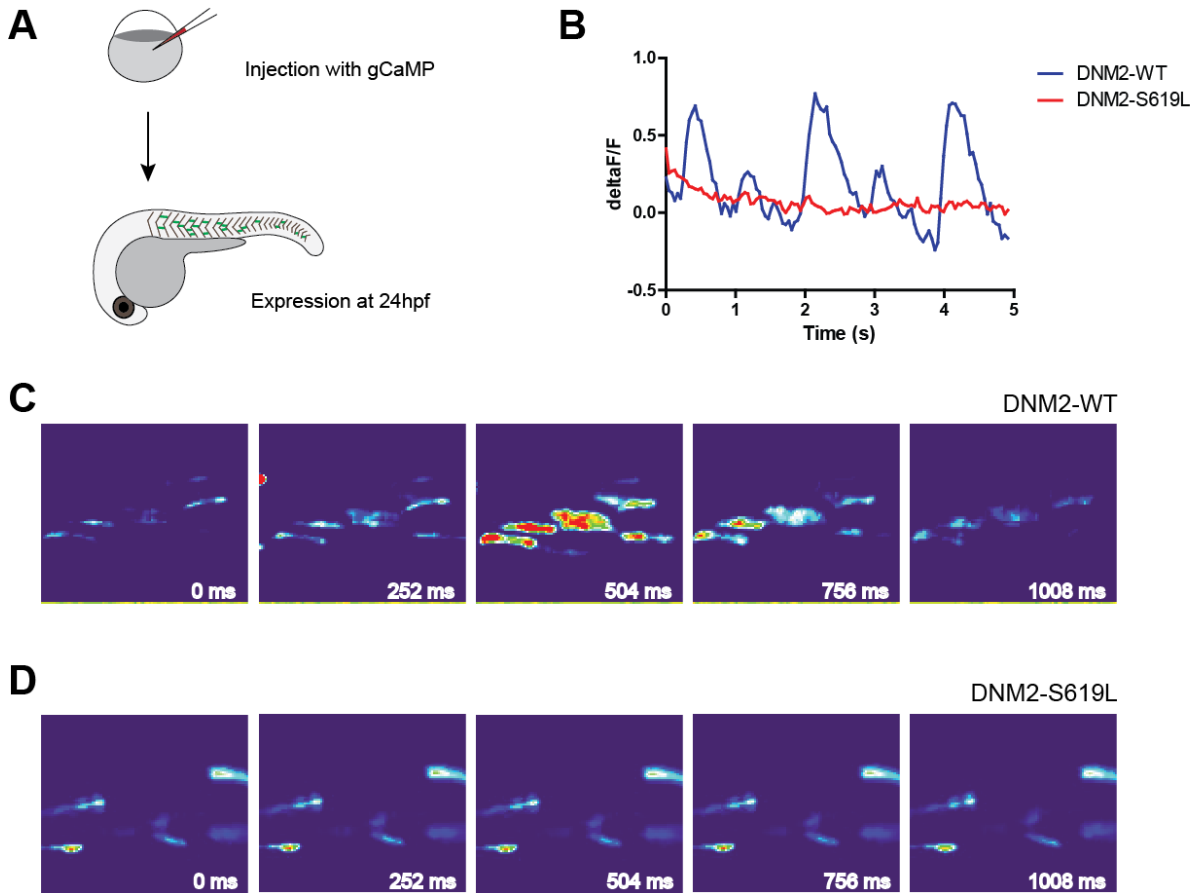


Figure 4-6: Calcium activity in DNM2-S619L larvae muscle.

(A) Injection of GCaMP, a genetically-encoded calcium indicator. Embryos were co-injected with GCaMP DNA and DNM2 RNA (WT or S619L). GCaMP muscle fluorescence was imaged during spontaneous muscle contractions at 24 hpf. (B) Representative trace of whole-embryo fluorescent intensity ($\Delta F/F$) during spontaneous contractions. Although DNM2-S619L larvae displayed spontaneous contractions with normal timing, there was no substantial increase in GCaMP fluorescence. (C-D) Sequential images of GCaMP fluorescence from the larvae in panel B.

4.4 Discussion

In this chapter, we present evidence for the role of DNM2 in t-tubule and SR organization. We show that myofibers from zebrafish with reduced *dnm2* expression have triads with atypical organization and an accumulation of excess membrane surrounding the SR. Notably, we find similar but non-identical membrane abnormalities in the muscle of larvae overexpressing DNM2-S619L. In DNM2-S619L larvae, there is substantial swelling of the SR and disorganized triads, as well as the presence of vacuole-like structures. In both models, some normal-appearing t-tubules are also present, suggesting that DNM2 is not essential for the initial establishment of t-tubule structures. This interpretation is consistent with the ultrastructural findings in a mouse model of DNM2-CNM, where DNM2-WT or DNM2-R465W was virally overexpressed in adult muscle [84]. The authors observed SR swelling and significant t-tubule abnormalities, despite the fact that mutant DNM2 was introduced into developed adult muscle and not present during initial myogenesis. Taken together with our findings in *dnm2* morphants and DNM2-S619L larvae, these results support a model in which DNM2 contributes to the long-term maintenance of muscle-specific organelles.

The difference in membrane phenotypes between reduced *dnm2* expression and DNM2-S619L overexpression also suggests that CNM-linked mutations do not simply abolish a muscle-specific function of DNM2. Intriguingly, a recent study showed that S619L and nearby mutations in DNM2 can cause an increase in *in vivo* GTPase activity and, in the case of the S619L mutation, render the protein insensitive to lipid stimulation [71]. While our findings do not necessarily point to specific biochemical changes in

DNM2 activity, an increase in GTPase activity is consistent with the fragmented tubules seen in our *ex vivo* tubulation experiments in COS cells.

In addition to demonstrating abnormal membrane organization in cells and zebrafish overexpressing DNM2-S619L, we show that calcium release is significantly reduced in myofibers from DNM2-S619L embryos. During spontaneous contractions, calcium levels were detected in individual myofibers using the genetically encoded calcium indicator GCaMP. Although muscle contractions were visible in all DNM2-S619L embryos that we examined, any calcium released was below the threshold of GCaMP detection. These data provide the first evidence for the dysregulation of calcium release in DNM2-CNM, and it is consistent with findings in other forms of CNM. Specifically, our lab previously demonstrated EC coupling defects in a zebrafish model of MTM1-CNM [74]. Similarly, Al-Qusairi et al. showed that myofibers from a MTM1 knockout mouse had EC coupling defects and decreased calcium transients [75]. Taken together with the data from our model of DNM2-CNM, these findings provide strong evidence that EC coupling defects are underlying pathomechanisms in all forms of CNM.

One key question that remains is the precise function of DNM2 in the maintenance of the sarcotubular network. DNM2 has a well-characterized role in shaping and remodeling membranes in non-muscle cells, but there is currently no evidence that it physically interacts with the t-tubule or SR. The gene products of *BINI*, *MTM1*, and *RYR1* have all been detected at the t-tubule by immunohistochemistry, but it remains unclear whether DNM2 localizes to this region. In view of the triad and EC coupling defects observed in *dnm2* knockdown and DNM2 disease models, it will be important to

determine if DNM2 is directly involved in modifying the t-tubule and SR, or if it has an indirect role in assembly and repair pathways.

4.5 Materials and Methods

Animal care: Zebrafish (AB strain) were bred and raised according to established protocols, under the guidelines of the University of Michigan Animal Care and Use protocols. Experiments were performed on zebrafish embryos and larvae between 1 and 2 dpf. All animals were handled in strict accordance with good animal practice as defined by national and local animal welfare bodies. All animal work was approved by the University of Michigan Committee for the Use and Care of Animals (UCUCA protocol #09835).

Analysis of motor behavior: Larvae were photographed using a Nikon AZ-100 microscope or a Leica MXIII stereoscope. Touch-evoked motor behaviors were elicited by touching the tail with a pair of No. 5 forceps. Speed measurements and video frame capture were performed using ImageJ (NIH).

Morpholino and RNA injection of zebrafish embryos: *dnm2* morphants and DNM2-S619L larvae were generated as described in Chapters 2 and 3. Briefly, fertilized eggs were collected after timed matings of adult zebrafish and injected at the 1–2-cell stage using a Nanoject II injector (Drummond Scientific). Embryos were injected with *dnm2* morpholino (.3 mM) or human DNM2 RNA (30 ng/μl) in a 4.6 nL volume.

Three-dimensional rendering of myofiber staining: Mixed cell cultures from 72 hpf embryos were isolated as previously described [74]. Briefly, larvae were dissociated in 10 mM collagenase type I (Sigma) for 60–90 min at room temperature. Embryos were

triturerated every 30 min. Dissociated preps were pelleted by centrifugation, resuspended in CO₂ independent media (Invitrogen), passed through a 70 mm filter (Falcon), and plated onto chamber slides (Falcon) precoated with poly-L-Lysine (Sigma). After 4 hours, cells were fixed for 15 min in 4% paraformaldehyde. Fixed cells were blocked in 10% NGS/0.3% Triton, incubated in mouse anti-DHPR1a (1:200; Abcam) overnight at 4°C, washed in PBS, incubated in secondary antibody (1:250; Invitrogen) washed in PBS, then mounted with ProLong Gold plus DAPI (Invitrogen). Z-stacks of 24 images were obtained by confocal microscopy, and three-dimensional rendering were constructed using Imaris software (Bitplane).

Muscle ultrastructure and semi-thin sections: For semi-thin sections, zebrafish were fixed overnight in Karnovsky's fixative at 3 dpf and then processed for embedding in epon by the Microscopy and Imaging Laboratory (MIL) core facility at the University of Michigan. Semi-thin sections were stained with toluidine blue and photographed using an Olympus BX43 microscope. Electron microscopy was performed by the MIL using a Phillips CM-100 transmission electron microscope.

***Ex vivo* tubulation in COS cells:** *Ex vivo* tubulation was performed following the basic methods described in [53]. The BIN1-GFP construct was a kind gift of Dr. Pietro De Camilli. COS7 cells were maintained in DMEM containing 1g/L glucose supplemented with 5% FBS. Cells were cultured on 22-mm² cover slips and were transfected with constructs expressing BIN1-GFP and DNM2-mCherry, using the *TransIT* reagent (Mirus). Cells were fixed with 4% paraformaldehyde for 15 min and then washed in PBS.

Measurements of calcium transients: The construct containing GCaMP under a muscle actin promoter was a kind gift of Dr. John Kuwada. Plasmid DNA was co-injected with DNM2 RNA at a concentration of 10ng/ μ L in 1-2 cell embryos. At 24 hours, embryos were embedded and immobilized in 1% low melt agarose. Fluorescent intensity during 10 seconds of spontaneous muscle contractions was recorded using a Nikon AZ-100 microscope. For image processing, ImageJ was used to measure total fluorescent intensity in a region of the larval trunk over the recorded interval. Baseline fluorescent levels were used to calculate relative fluorescence ($\Delta F/F$).

Statistical analysis: Statistical analysis was performed on data using the GraphPad Prism 5 software package. Significance was determined using Student's t-test or Fisher's exact test.

Chapter 5: Conclusions and Future Directions

The results described in this dissertation suggest that CNM-associated mutations in DNM2 alter function at two key regions of the muscle fiber: the post-synaptic NMJ and the sarcotubular network. Specifically, in DNM2-S619L fish, we find evidence of structural and functional defects in both of these regions. Our findings, combined with evidence from other forms of centronuclear myopathy, point to possible pathogenic changes that may underlie muscle weakness in patients with DNM2-CNM.

With this outcome in mind, it is important to consider what might lead to membrane abnormalities at both the post-synaptic NMJ and sarcotubular network. In terms of the chemical and excitatory events that lead to muscle contraction, these two regions have distinct functions. However, they share important characteristics in terms of membrane organization. At the NMJ, invaginations of the plasma membrane form junctional folds, which make up a network known as the secondary synaptic cleft. Like t-tubules, these membranes structures extend the surface area of the plasma membrane and serve as the location for key receptors and channels. Both t-tubules and junctional folds require efficient receptor delivery and turnover, and both have a highly specific membrane architecture that needs to be maintained in the context of rapid muscle fiber contraction and relaxation.

Given these shared characteristics, it is reasonable to hypothesize that both the NMJ and sarco-tubular network place heavy - and perhaps unique - demands on dynamin-dependent pathways. It will be important for future studies to clarify the exact nature of this role. It has been suggested that DNM2 might be directly involved in shaping the plasma membrane into t-tubules, in a pathway similar to the membrane deformation coordinated by DNM2 and amphiphysin-2 during clathrin-mediated endocytosis [53, 58]. Amphiphysin- 2 has a known role in t-tubule formation [72, 73], but whether it also interacts with DNM2 at the t-tubule has yet to be determined.

In one potential model of t-tubule formation, DNM2 helical assemblies act on plasma membrane and shape t-tubules through GTP-dependent torsion. There is little direct evidence for this role, and it has been argued that the biophysical arrangement of DNM2 oligomers is not appropriate for forming structures the size of t-tubules [84]. Our results imply that Dnm2 is not essential for primary t-tubule biogenesis in zebrafish, since t-tubules are present in *dnm2*-deficient muscle. However, DNM2 has a wide spectrum of functions in membrane trafficking pathways, and it also interacts extensively with components of actin and microtubule networks [2-11]. Even if DNM2 does not directly participate in deforming membranes to form t-tubules, there are a variety of roles that it could play in establishing or maintaining these structures. DNM2-dependent pathways may donate membrane to nascent t-tubules during development, or they might recycle membrane components in mature t-tubules. Some key questions about the basic formation of t-tubules have yet to be answered [108], and further research into the mechanisms that shape these organelles will likely provide insight into the specific function of DNM2.

To better understand DNM2-related muscle disease, identifying the role of dynamin-2 in normal mammalian myogenesis will be important. A conditional *Dnm2* knockout mouse is commercially available through Jackson Laboratories, and the generation of a muscle-specific knockout mouse would be a valuable tool for future study. Examining myogenesis in the absence of DNM2 would clarify the requirement for DNM2 in t-tubule biogenesis and could potentially establish a broader role for DNM2 in muscle biology.

In order to examine the pathogenesis of DNM2-CNM, we generated zebrafish expressing human DNM2-S619L. DNM2-S619L fish recapitulate key features of human DNM2-CNM, including defects in motor behavior and membrane disorganization surrounding muscle nuclei. These findings contrast with the mild phenotype of the DNM2-R465W knockin mouse, which is currently the only genetic mouse model for DNM2-CNM [85]. These mice have no motor abnormalities and do not share any of the major histopathologic changes associated with DNM2-CNM. Our zebrafish model therefore addresses an important gap in the literature.

Since expression of injected RNA decreases over time, our study of DNM2-S619L fish is limited to the first three days of development. However, our results show that useful and disease-relevant assays can be performed within this developmental window. At 3 dpf, we demonstrate defects in motor behavior and successfully treat developing larvae with a pharmacological agent. In several respects, a transient model of disease can also offer advantages over a germline transgenic model. It is fast and relatively inexpensive to inject embryos with RNA, and there is no need to maintain a special transgenic line. This makes the zebrafish an appealing model in which to rapidly test the effect of other DNM2 mutations. The full experiment - generation of RNA, injection of

embryos and screening of larvae - can take place within a few days, as opposed to the months required for generating a transgenic zebrafish or mouse. This approach could allow the quick testing of novel mutations identified in patients with DNM2-CNM, and it could also help clarify the role of single nucleotide polymorphisms with undetermined pathogenicity.

Based on the robust phenotype of the transient DNM2-S619L fish, the generation of a stable DNM2-S619L transgenic fish is a logical next step. A transgenic zebrafish model would facilitate a number of experiments that could expand the findings we observe in our transient model. In particular, it would allow the examination of muscle histology and motor behavior in juvenile and adult fish. A transgenic line would also provide a useful platform for medium or high throughput drug screens, since large numbers of embryos could be generated with stable expression of human DNM2-S619L.

Since the DNM2-S619L mutation is associated with severe muscle weakness early in life, it may prove difficult to generate a viable transgenic line carrying this mutation. A conditional transgenic approach would be more likely to produce a successful transgenic line. The heat shock promoter has been used in zebrafish to express a variety of transgenes [109]. This strategy would be particularly useful for modeling DNM2-CNM, since it allows the gene to be turned on at any point in development. Since viral overexpression of mutant DNM2 in adult mouse muscle causes a CNM-like phenotype [84], the disease phenotype in DNM2-CNM may not be related to early muscle development. A conditional DNM2-S619L zebrafish would provide a valuable tool for dissecting the temporal dynamics of pathogenesis in DNM2-CNM.

This dissertation describes the second zebrafish model of a human centronuclear myopathy, following the characterization of a transient zebrafish model of myotubular myopathy [74]. Both of these models have provided novel insights into their respective human disorders. *Mtm1*-deficient zebrafish provided the first evidence that t-tubule defects and aberrant EC coupling are a feature of myotubular myopathy, which is supported by evidence in human patients and mammalian models CNM [57, 75, 76]. Using DNM2-S619L fish, we show that neuromuscular junction defects may be a component of DNM2-CNM. This observation is supported by case studies of two patients with DNM2-CNM. Together, these findings in *mtm1*-deficient and DNM2-S619L larvae show that the zebrafish is a powerful system for examining pathogenesis in centronuclear myopathies. As additional CNM-causing genes are identified, it will be worthwhile to consider strategies for modeling these disorders in the zebrafish.

In addition to identifying pathways that may underlie muscle weakness in DNM2-CNM patients, the work presented in this dissertation also points to a potential drug therapy. DNM2-S619L zebrafish have substantial muscle weakness, as evinced by their slow escape responses and restricted tail beats. This weakness is rapidly and substantially alleviated by treatment with a short-acting acetylcholinesterase inhibitor. Retrospective analysis of two patients with DNM2-CNM showed that both patients reported symptomatic improvement after starting acetylcholinesterase inhibitor treatment. This is the first report of acetylcholinesterase treatment in patients with genetically confirmed DNM2-CNM. Currently, there are no standard drug therapies used in the clinical management of centronuclear myopathies. Our data, combined with previous reports of patients with genetically uncharacterized centronuclear myopathy, point to a

therapeutic with the potential to substantially improve quality of life for patients. Clinical trials of acetylcholinesterase inhibitors are an essential next step for validating this therapy in patients with DNM2-CNM and related disorders.

In conclusion, the results described in this dissertation provide a significant contribution to the current understanding of DNM2-CNM. We demonstrate that DNM2-S619L fish are a biologically-relevant model for DNM2-CNM, and that two different pathomechanisms may directly contribute to muscle weakness in this disorder. We also identify a class of drugs with therapeutic potential for patients with DNM2-CNM. There are still key questions that remain regarding mechanisms of disease in DNM2-CNM, and in the centronuclear myopathies as a group. The research described here provides new insights and novel tools for addressing these questions, and we look forward to applying these results in order to benefit patients with centronuclear myopathy.

Bibliography

1. Praefcke, G.J. and H.T. McMahon, *The dynamin superfamily: universal membrane tubulation and fission molecules?* Nat Rev Mol Cell Biol, 2004. **5**(2): p. 133-47.
2. Jones, S.M., et al., *Role of dynamin in the formation of transport vesicles from the trans-Golgi network.* Science, 1998. **279**(5350): p. 573-7.
3. Gold, E.S., et al., *Dynamin 2 is required for phagocytosis in macrophages.* J Exp Med, 1999. **190**(12): p. 1849-56.
4. Cao, H., et al., *Dynamin 2 mediates fluid-phase micropinocytosis in epithelial cells.* J Cell Sci, 2007. **120**(Pt 23): p. 4167-77.
5. Thompson, H.M., et al., *The large GTPase dynamin associates with the spindle midzone and is required for cytokinesis.* Curr Biol, 2002. **12**(24): p. 2111-7.
6. Thompson, H.M., et al., *Dynamin 2 binds gamma-tubulin and participates in centrosome cohesion.* Nat Cell Biol, 2004. **6**(4): p. 335-42.
7. McNiven, M.A., et al., *Regulated interactions between dynamin and the actin-binding protein cortactin modulate cell shape.* J Cell Biol, 2000. **151**(1): p. 187-98.
8. Orth, J.D., et al., *The large GTPase dynamin regulates actin comet formation and movement in living cells.* Proc Natl Acad Sci U S A, 2002. **99**(1): p. 167-72.

9. Schafer, D.A., et al., *Dynamin2 and cortactin regulate actin assembly and filament organization*. *Curr Biol*, 2002. **12**(21): p. 1852-7.
10. Ferguson, S.M., et al., *Coordinated actions of actin and BAR proteins upstream of dynamin at endocytic clathrin-coated pits*. *Dev Cell*, 2009. **17**(6): p. 811-22.
11. Gu, C., et al., *Direct dynamin-actin interactions regulate the actin cytoskeleton*. *Embo J*, 2010. **29**(21): p. 3593-606.
12. Diatloff-Zito, C., et al., *Isolation of an ubiquitously expressed cDNA encoding human dynamin II, a member of the large GTP-binding protein family*. *Gene*, 1995. **163**(2): p. 301-6.
13. Cook, T.A., R. Urrutia, and M.A. McNiven, *Identification of dynamin 2, an isoform ubiquitously expressed in rat tissues*. *Proc Natl Acad Sci U S A*, 1994. **91**(2): p. 644-8.
14. Sontag, J.M., et al., *Differential expression and regulation of multiple dynamins*. *J Biol Chem*, 1994. **269**(6): p. 4547-54.
15. Nakata, T., R. Takemura, and N. Hirokawa, *A novel member of the dynamin family of GTP-binding proteins is expressed specifically in the testis*. *J Cell Sci*, 1993. **105 (Pt 1)**: p. 1-5.
16. Shpetner, H.S. and R.B. Vallee, *Identification of dynamin, a novel mechanochemical enzyme that mediates interactions between microtubules*. *Cell*, 1989. **59**(3): p. 421-32.
17. van der Blik, A.M., et al., *Mutations in human dynamin block an intermediate stage in coated vesicle formation*. *J Cell Biol*, 1993. **122**(3): p. 553-63.

18. Takei, K., et al., *Tubular membrane invaginations coated by dynamin rings are induced by GTP-gamma S in nerve terminals*. Nature, 1995. **374**(6518): p. 186-90.
19. Kozlov, M.M., *Dynamin: possible mechanism of "Pinchase" action*. Biophys J, 1999. **77**(1): p. 604-16.
20. Marks, B., et al., *GTPase activity of dynamin and resulting conformation change are essential for endocytosis*. Nature, 2001. **410**(6825): p. 231-5.
21. Faelber, K., et al., *Crystal structure of nucleotide-free dynamin*. Nature, 2011. **477**(7366): p. 556-60.
22. Ford, M.G., S. Jenni, and J. Nunnari, *The crystal structure of dynamin*. Nature, 2011. **477**(7366): p. 561-6.
23. Muhlberg, A.B., D.E. Warnock, and S.L. Schmid, *Domain structure and intramolecular regulation of dynamin GTPase*. Embo J, 1997. **16**(22): p. 6676-83.
24. Smirnova, E., et al., *A model for dynamin self-assembly based on binding between three different protein domains*. J Biol Chem, 1999. **274**(21): p. 14942-7.
25. Ramachandran, R., et al., *The dynamin middle domain is critical for tetramerization and higher-order self-assembly*. Embo J, 2007. **26**(2): p. 559-66.
26. Gout, I., et al., *The GTPase dynamin binds to and is activated by a subset of SH3 domains*. Cell, 1993. **75**(1): p. 25-36.
27. Shpetner, H.S., J.S. Herskovits, and R.B. Vallee, *A binding site for SH3 domains targets dynamin to coated pits*. J Biol Chem, 1996. **271**(1): p. 13-6.

28. Tuma, P.L., M.C. Stachniak, and C.A. Collins, *Activation of dynamin GTPase by acidic phospholipids and endogenous rat brain vesicles*. J Biol Chem, 1993. **268**(23): p. 17240-6.
29. Salim, K., et al., *Distinct specificity in the recognition of phosphoinositides by the pleckstrin homology domains of dynamin and Bruton's tyrosine kinase*. Embo J, 1996. **15**(22): p. 6241-50.
30. Zheng, J., et al., *Identification of the binding site for acidic phospholipids on the pH domain of dynamin: implications for stimulation of GTPase activity*. J Mol Biol, 1996. **255**(1): p. 14-21.
31. Dong, J., et al., *Expression and purification of dynamin II domains and initial studies on structure and function*. Protein Expr Purif, 2000. **20**(2): p. 314-23.
32. Bethoney, K.A., et al., *A possible effector role for the pleckstrin homology (PH) domain of dynamin*. Proc Natl Acad Sci U S A, 2009. **106**(32): p. 13359-64.
33. Ramachandran, R., et al., *Membrane insertion of the pleckstrin homology domain variable loop 1 is critical for dynamin-catalyzed vesicle scission*. Mol Biol Cell, 2009. **20**(22): p. 4630-9.
34. Zuchner, S., et al., *Mutations in the pleckstrin homology domain of dynamin 2 cause dominant intermediate Charcot-Marie-Tooth disease*. Nat Genet, 2005. **37**(3): p. 289-94.
35. Bitoun, M., et al., *Mutations in dynamin 2 cause dominant centronuclear myopathy*. Nat Genet, 2005. **37**(11): p. 1207-9.
36. Jeannet, P.Y., et al., *Clinical and histologic findings in autosomal centronuclear myopathy*. Neurology, 2004. **62**(9): p. 1484-90.

37. Bitoun, M., et al., *A new centronuclear myopathy phenotype due to a novel dynamin 2 mutation*. *Neurology*, 2009. **72**(1): p. 93-5.
38. Susman, R.D., et al., *Expanding the clinical, pathological and MRI phenotype of DNM2-related centronuclear myopathy*. *Neuromuscul Disord*, 2010. **20**(4): p. 229-37.
39. Hanisch, F., et al., *Phenotype variability and histopathological findings in centronuclear myopathy due to DNM2 mutations*. *J Neurol*, 2011. **258**(6): p. 1085-90.
40. Liewluck, T., et al., *Sporadic centronuclear myopathy with muscle pseudohypertrophy, neutropenia, and necklace fibers due to a DNM2 mutation*. *Neuromuscul Disord*, 2010. **20**(12): p. 801-4.
41. Bitoun, M., et al., *A novel mutation in the dynamin 2 gene in a Charcot-Marie-Tooth type 2 patient: clinical and pathological findings*. *Neuromuscul Disord*, 2008. **18**(4): p. 334-8.
42. Fischer, D., et al., *Characterization of the muscle involvement in dynamin 2-related centronuclear myopathy*. *Brain*, 2006. **129**(Pt 6): p. 1463-9.
43. Echaniz-Laguna, A., et al., *Subtle central and peripheral nervous system abnormalities in a family with centronuclear myopathy and a novel dynamin 2 gene mutation*. *Neuromuscul Disord*, 2007. **17**(11-12): p. 955-9.
44. Jeub, M., et al., *Dynamin 2-related centronuclear myopathy: clinical, histological and genetic aspects of further patients and review of the literature*. *Clin Neuropathol*, 2008. **27**(6): p. 430-8.

45. Claeys, K.G., et al., *Phenotypic spectrum of dynamin 2 mutations in Charcot-Marie-Tooth neuropathy*. Brain, 2009. **132**(Pt 7): p. 1741-52.
46. Jungbluth, H., et al., *Centronuclear myopathy with cataracts due to a novel dynamin 2 (DNM2) mutation*. Neuromuscul Disord, 2010. **20**(1): p. 49-52.
47. Laporte, J., et al., *A gene mutated in X-linked myotubular myopathy defines a new putative tyrosine phosphatase family conserved in yeast*. Nat Genet, 1996. **13**(2): p. 175-82.
48. Cao, C., et al., *Sequential actions of myotubularin lipid phosphatases regulate endosomal PI(3)P and growth factor receptor trafficking*. Mol Biol Cell, 2008. **19**(8): p. 3334-46.
49. Cao, C., et al., *Myotubularin lipid phosphatase binds the hVPS15/hVPS34 lipid kinase complex on endosomes*. Traffic, 2007. **8**(8): p. 1052-67.
50. Jungbluth, H., C. Wallgren-Pettersson, and J. Laporte, *Centronuclear (myotubular) myopathy*. Orphanet J Rare Dis, 2008. **3**: p. 26.
51. Herman, G.E., et al., *Characterization of mutations in fifty North American patients with X-linked myotubular myopathy*. Hum Mutat, 2002. **19**(2): p. 114-21.
52. McEntagart, M., et al., *Genotype-phenotype correlations in X-linked myotubular myopathy*. Neuromuscul Disord, 2002. **12**(10): p. 939-46.
53. Nicot, A.S., et al., *Mutations in amphiphysin 2 (BIN1) disrupt interaction with dynamin 2 and cause autosomal recessive centronuclear myopathy*. Nat Genet, 2007. **39**(9): p. 1134-9.

54. Mejaddam, A.Y., I. Nennesmo, and T. Sejersen, *Severe phenotype of a patient with autosomal recessive centronuclear myopathy due to a BIN1 mutation*. Acta Myol, 2009. **28**(3): p. 91-3.
55. Bohm, J., et al., *Case report of intrafamilial variability in autosomal recessive centronuclear myopathy associated to a novel BIN1 stop mutation*. Orphanet J Rare Dis, 2010. **5**: p. 35.
56. Claeys, K.G., et al., *Phenotype of a patient with recessive centronuclear myopathy and a novel BIN1 mutation*. Neurology, 2010. **74**(6): p. 519-21.
57. Toussaint, A., et al., *Defects in amphiphysin 2 (BIN1) and triads in several forms of centronuclear myopathies*. Acta Neuropathol, 2011. **121**(2): p. 253-66.
58. Takei, K., et al., *Functional partnership between amphiphysin and dynamin in clathrin-mediated endocytosis*. Nat Cell Biol, 1999. **1**(1): p. 33-9.
59. Jungbluth, H., et al., *Centronuclear myopathy due to a de novo dominant mutation in the skeletal muscle ryanodine receptor (RYR1) gene*. Neuromuscul Disord, 2007. **17**(4): p. 338-45.
60. Wilmshurst, J.M., et al., *RYR1 mutations are a common cause of congenital myopathies with central nuclei*. Ann Neurol, 2010. **68**(5): p. 717-26.
61. Bevilacqua, J.A., et al., *Recessive RYR1 mutations cause unusual congenital myopathy with prominent nuclear internalization and large areas of myofibrillar disorganization*. Neuropathol Appl Neurobiol, 2011. **37**(3): p. 271-84.
62. Tosch, V., et al., *A novel PtdIns3P and PtdIns(3,5)P2 phosphatase with an inactivating variant in centronuclear myopathy*. Hum Mol Genet, 2006. **15**(21): p. 3098-106.

63. Dowling, J.J., et al., *Zebrafish MTMR14 is required for excitation-contraction coupling, developmental motor function and the regulation of autophagy*. Hum Mol Genet, 2010. **19**(13): p. 2668-81.
64. Gibbs, E.M., E.L. Feldman, and J.J. Dowling, *The role of MTMR14 in autophagy and in muscle disease*. Autophagy, 2010. **6**(6): p. 819-20.
65. Tanabe, K. and K. Takei, *Dynamic instability of microtubules requires dynamin 2 and is impaired in a Charcot-Marie-Tooth mutant*. J Cell Biol, 2009. **185**(6): p. 939-48.
66. Bitoun, M., et al., *Dynamin 2 mutations associated with human diseases impair clathrin-mediated receptor endocytosis*. Hum Mutat, 2009. **30**(10): p. 1419-27.
67. Koutsopoulos, O.S., et al., *Mild functional differences of dynamin 2 mutations associated to centronuclear myopathy and charcot-marie-tooth peripheral neuropathy*. PLoS One, 2011. **6**(11): p. e27498.
68. Liu, Y.W., V. Lukiyanchuk, and S.L. Schmid, *Common membrane trafficking defects of disease-associated dynamin 2 mutations*. Traffic, 2011. **12**(11): p. 1620-33.
69. Fish, K.N., S.L. Schmid, and H. Damke, *Evidence that dynamin-2 functions as a signal-transducing GTPase*. J Cell Biol, 2000. **150**(1): p. 145-54.
70. Wang, L., et al., *Dynamin 2 mutants linked to centronuclear myopathies form abnormally stable polymers*. J Biol Chem, 2010. **285**(30): p. 22753-7.
71. Kenniston, J.A. and M.A. Lemmon, *Dynamin GTPase regulation is altered by PH domain mutations found in centronuclear myopathy patients*. Embo J, 2010. **29**(18): p. 3054-67.

72. Lee, E., et al., *Amphiphysin 2 (Bin1) and T-tubule biogenesis in muscle*. Science, 2002. **297**(5584): p. 1193-6.
73. Razzaq, A., et al., *Amphiphysin is necessary for organization of the excitation-contraction coupling machinery of muscles, but not for synaptic vesicle endocytosis in Drosophila*. Genes Dev, 2001. **15**(22): p. 2967-79.
74. Dowling, J.J., et al., *Loss of myotubularin function results in T-tubule disorganization in zebrafish and human myotubular myopathy*. PLoS Genet, 2009. **5**(2): p. e1000372.
75. Al-Qusairi, L., et al., *T-tubule disorganization and defective excitation-contraction coupling in muscle fibers lacking myotubularin lipid phosphatase*. Proc Natl Acad Sci U S A, 2009. **106**(44): p. 18763-8.
76. Beggs, A.H., et al., *MTM1 mutation associated with X-linked myotubular myopathy in Labrador Retrievers*. Proc Natl Acad Sci U S A, 2010. **107**(33): p. 14697-702.
77. Sher, J.H., et al., *Familial centronuclear myopathy: a clinical and pathological study*. Neurology, 1967. **17**(8 Pt 1): p. 727-42.
78. Harriman, D.G. and M.A. Haleem, *Centronuclear myopathy in old age*. J Pathol, 1972. **108**(3): p. 237-47.
79. Elder, G.B., et al., *Infantile centronuclear myopathy. Evidence suggesting incomplete innervation*. J Neurol Sci, 1983. **60**(1): p. 79-88.
80. Fidzianska, A. and H.H. Goebel, *Aberrant arrested in maturation neuromuscular junctions in centronuclear myopathy*. J Neurol Sci, 1994. **124**(1): p. 83-8.

81. Engel, A., *Myasthenia gravis and myasthenic disorders*. 1999, New York ; Oxford: Oxford University Press. xx, 310 p. [1] p of plates.
82. Liewluck, T., et al., *Endplate structure and parameters of neuromuscular transmission in sporadic centronuclear myopathy associated with myasthenia*. Neuromuscul Disord, 2011. **21**(6): p. 387-95.
83. Robb, S.A., et al., *Impaired neuromuscular transmission and response to acetylcholinesterase inhibitors in centronuclear myopathies*. Neuromuscul Disord, 2011. **21**(6): p. 379-86.
84. Cowling, B.S., et al., *Increased expression of wild-type or a centronuclear myopathy mutant of dynamin 2 in skeletal muscle of adult mice leads to structural defects and muscle weakness*. Am J Pathol, 2011. **178**(5): p. 2224-35.
85. Durieux, A.C., et al., *A centronuclear myopathy-dynamin 2 mutation impairs skeletal muscle structure and function in mice*. Hum Mol Genet, 2010. **19**(24): p. 4820-36.
86. Pucadyil, T.J. and S.L. Schmid, *Conserved functions of membrane active GTPases in coated vesicle formation*. Science, 2009. **325**(5945): p. 1217-20.
87. Henley, J.R., et al., *Dynamin-mediated internalization of caveolae*. J Cell Biol, 1998. **141**(1): p. 85-99.
88. Ahn, H.J., et al., *The expression profile and function of Satb2 in zebrafish embryonic development*. Mol Cells, 2010. **30**(4): p. 377-82.
89. Kida, Y.S., et al., *Daam1 regulates the endocytosis of EphB during the convergent extension of the zebrafish notochord*. Proc Natl Acad Sci U S A, 2007. **104**(16): p. 6708-13.

90. Feng, B., H. Schwarz, and S. Jesuthasan, *Furrow-specific endocytosis during cytokinesis of zebrafish blastomeres*. *Exp Cell Res*, 2002. **279**(1): p. 14-20.
91. Taylor, J.S., et al., *Genome duplication, a trait shared by 22000 species of ray-finned fish*. *Genome Res*, 2003. **13**(3): p. 382-90.
92. Postlethwait, J., et al., *Subfunction partitioning, the teleost radiation and the annotation of the human genome*. *Trends Genet*, 2004. **20**(10): p. 481-90.
93. Naruse, K., et al., *A medaka gene map: the trace of ancestral vertebrate proto-chromosomes revealed by comparative gene mapping*. *Genome Res*, 2004. **14**(5): p. 820-8.
94. Long, Q.M., et al., *GATA-1 expression pattern can be recapitulated in living transgenic zebrafish using GFP reporter gene*. *Development*, 1997. **124**(20): p. 4105-4111.
95. Daniels, G.D. and C.J. Secombes, *Genomic organisation of rainbow trout, *Oncorhynchus mykiss* TGF-beta*. *Dev Comp Immunol*, 1999. **23**(2): p. 139-47.
96. Pugacheva, E.M., et al., *Cloning and characterization of zebrafish CTCF: Developmental expression patterns, regulation of the promoter region, and evolutionary aspects of gene organization*. *Gene*, 2006. **375**: p. 26-36.
97. Kwan, K.M., et al., *The Tol2kit: a multisite gateway-based construction kit for Tol2 transposon transgenesis constructs*. *Dev Dyn*, 2007. **236**(11): p. 3088-99.
98. Achiriloaie, M., B. Barylko, and J.P. Albanesi, *Essential role of the dynamin pleckstrin homology domain in receptor-mediated endocytosis*. *Mol Cell Biol*, 1999. **19**(2): p. 1410-5.

99. Kruchten, A.E. and M.A. McNiven, *Dynamin as a mover and pincher during cell migration and invasion*. J Cell Sci, 2006. **119**(Pt 9): p. 1683-90.
100. Nicholson, G. and S. Myers, *Intermediate forms of Charcot-Marie-Tooth neuropathy: a review*. Neuromolecular Med, 2006. **8**(1-2): p. 123-30.
101. Orth, J.D. and M.A. McNiven, *Dynamin at the actin-membrane interface*. Curr Opin Cell Biol, 2003. **15**(1): p. 31-9.
102. Schafer, D.A., *Regulating actin dynamics at membranes: a focus on dynamin*. Traffic, 2004. **5**(7): p. 463-9.
103. Bitoun, M., et al., *Dynamin 2 mutations cause sporadic centronuclear myopathy with neonatal onset*. Ann Neurol, 2007. **62**(6): p. 666-70.
104. Cartaud, A., et al., *Agrin triggers the clustering of raft-associated acetylcholine receptors through actin cytoskeleton reorganization*. Biol Cell, 2011. **103**(6): p. 287-301.
105. Moransard, M., et al., *Agrin regulates rapsyn interaction with surface acetylcholine receptors, and this underlies cytoskeletal anchoring and clustering*. J Biol Chem, 2003. **278**(9): p. 7350-9.
106. Okamoto, P.M., et al., *Dynamin isoform-specific interaction with the shank/ProSAP scaffolding proteins of the postsynaptic density and actin cytoskeleton*. J Biol Chem, 2001. **276**(51): p. 48458-65.
107. Westerfield, M., *The zebrafish book : a guide for the laboratory use of zebrafish (Brachydanio rerio)*. 1993, Eugene, OR: M. Westerfield.
108. Al-Qusairi, L. and J. Laporte, *T-tubule biogenesis and triad formation in skeletal muscle and implication in human diseases*. Skelet Muscle, 2011. **1**(1): p. 26.

109. Shoji, W. and M. Sato-Maeda, *Application of heat shock promoter in transgenic zebrafish*. *Dev Growth Differ*, 2008. **50**(6): p. 401-6.